

Evolution and determinants of firm-level systemic risk in local production networks

Anna Mancini^{1,2,*}, Balázs Lengyel^{3,4,5}, Riccardo Di Clemente^{6,7}, and Giulio Cimini^{1,2,8}

¹Physics Department and INFN, University of Rome Tor Vergata, 00133 Rome (Italy)

²Enrico Fermi Research Center, 00184 Rome (Italy)

³Agglomeration, Networks and Innovation MTA Momentum Research Group, HUN-REN Centre for Economic and Regional Studies, 1097 Budapest (Hungary)

⁴ANETI Lab, Corvinus Institute for Advanced Studies, Corvinus University of Budapest, 1093 Budapest (Hungary)

⁵Department of Network Science, Institute for Data Analytics and Information Systems, Corvinus University of Budapest, 1093 Budapest (Hungary)

⁶Complex Connections Lab, Network Science Institute, Northeastern University London, London E1W 1LP (United Kingdom)

⁷ISI Foundation, Via Chisola 5, 10126 Turin (Italy)

⁸Institute for Complex Systems, National Research Council, 00185 Rome (Italy)

*anna.mancini@cref.it

ABSTRACT

Recent crises like the COVID-19 pandemic and geopolitical tensions have exposed vulnerabilities and caused disruptions of supply chains, leading to product shortages, increased costs, and economic instability. This has prompted increasing efforts to assess systemic risk, namely the effects of firm disruptions on entire economies. However, the ability of firms to react to crises by rewiring their supply links has been largely overlooked, limiting our understanding of production networks resilience. Here we study dynamics and determinants of firm-level systemic risk in the Hungarian production network from 2015 to 2022. We use as benchmark a heuristic maximum entropy null model that generates an ensemble of production networks at equilibrium, by preserving the total input (demand) and output (supply) of each firm at the sector level. We show that the fairly stable set of firms with highest systemic risk undergoes a structural change during COVID-19, as those enabling economic exchanges become key players in the economy – a result which is not reproduced by the null model. Although the empirical systemic risk aligns well with the null value until the onset of the pandemic, it becomes significantly smaller afterwards as the adaptive behavior of firms leads to a more resilient economy. Furthermore, firms' international trade volume (being a subject of disruption) becomes a significant predictor of their systemic risk. However, international links cannot provide an unequivocal explanation for the observed trends, as imports and exports have opposing effects on local systemic risk through the supply and demand channels.

Introduction

Production networks arise as firms exchange goods and services that are needed for their own production^{1,2}. The resulting interdependencies between suppliers, manufacturers, and consumers in industries and geographic regions amplify economic and technological progress and are crucial to the functioning of modern economies^{3,4}. However, production networks have become increasingly vulnerable^{5,6}, as a consequence of the growing globalization, interconnectedness, and complexity of supply chains^{7,8} as well as the constant effort toward efficiency⁹. Interconnectedness, in particular, means that disruptions affecting firms in one region or sector can ripple across the entire network, with large-scale economic consequences¹⁰. The propagation of shocks through global supply chains has occurred several times recently. For example, natural disasters such as Hurricane Katrina and the Fukushima earthquake had economic impacts far beyond the area directly affected^{11–13}. Similarly, geopolitical events, such as the Russian invasion of Ukraine, disrupted global grain supplies for the importing nations¹⁴. In the paramount case of the COVID-19 pandemic, the lockdown measures and subsequent factory shutdowns had a disruptive effect on global production networks, impacting entire economies that have been unable to supply basic goods to the population^{15–19}. These events have triggered a growing interest in assessing systemic risk – specifically, understanding how disruptions can propagate through production networks and cause large-scale economic effects, and how local networks face external shocks through their export and import connections.

Although the propagation of economic shocks has traditionally been studied using industry-level Input-Output tables^{20–23}, recently the attention has shifted to production networks at the firm level^{24–26}, due to the availability of large-scale datasets of

inter-firm relationships²⁷. Notably, the use of firm-level data allows to overcome the aggregation bias of Input-Output tables²⁸ and to obtain more reliable estimates of systemic risk²⁹. The supply chain management literature studied several aspects about the spreading of disruptions along supply chains, such as the *supply chain resilience*³⁰, the *snowball effect*³¹, the *ripple effect*³² and the *nexus suppliers* index³³, recognizing the importance of considering variability³⁴ and topological features³⁵ of the underlying network. Furthermore, how supplier and customer disruptions affect firms depends on their production process and network position. The recently proposed *Economic Systemic Risk Index* (ESRI)³⁶ builds on this know-how to evaluate the riskiness of a firm in terms of the total reduction in output experienced by the economy as a consequence of its failure.

Measuring systemic risk typically relies on a static network assumption, where firms and their relationships within the production network are fixed as shocks propagate. This allows simplifying the analysis and is useful for devising strategies to enhance resilience (e.g., diversifying suppliers, stockpiling resources, investing in redundant infrastructure). However, when a crisis occurs, firms actively respond by adapting their supply chains^{37–40}. These adaptations can involve finding alternative suppliers, changing logistics pathways, reallocating production, or taking advantage of new market opportunities that arise during the crisis^{41–44}. Such adaptive responses are not just temporary fixes but can lead to long-term modifications in the structure of the production network^{45,46}. These changes can then either dampen systemic risk by making the network more resilient and diversified or, in some cases, exacerbate it by creating new dependencies and bottlenecks. As a result, systemic risk is no longer a static property that can be measured solely based on the pre-crisis network structure.

In this work, we study the evolution and determinants of firm-level systemic risk using the Hungarian production network (see Methods), which contains all firms and all their value-added tax (VAT) interactions during years from 2015 to 2022 – thus including the outbreak of the COVID-19 pandemic. We compute and trace the ESRI value for each firm in the network (see Methods) to draw a detailed portrait of the evolution of systemic risk at the individual firm and sector level over a wide time span. This enables us to investigate, for the first time, how resilience evolves throughout the years, obtaining a comprehensive analysis of system-level adaptation to the COVID-19 shock and identifying new key players of the economy. We are particularly interested in understanding how firms' attributes – including international trade linkages – and their specific position in the evolving complex production network determine their systemic risk properties. To focus on this aspect, we benchmark empirical findings to a null network model that incorporates individual characteristics of firms.

In the context of networks, unbiased null models can be defined within the framework of Exponential Random Graphs (ERGs), rooted in the Maximum Entropy principle^{47,48}. The idea is to generate an ensemble of networks that are maximally random but preserve (constrain) specific quantities of the empirical network. These models can then be used to define a rigorous null hypothesis that the imposed constraints can explain any observation on the network (see e.g. ^{49–53}). Here we use the *stripe-corrected gravity model* (s-GM)⁵⁴, a recent heuristic formulation for production networks that constrains the input and output flow of each firm by sector, and generates sparse networks using a fitness assumption that firms' connectivity is proportional to size (see Methods). We employ the s-GM to generate an ensemble of networks over which we compute ESRI scores, serving as null values against which we can assess our empirical findings. Note that the s-GM has already been shown to capture well the ESRI of individual firms during normal times⁵⁵.

By constraining the supply and demand of each firm by sector, the s-GM is in line with the assumption of fixed production function and input portfolio (here proxied by sectors) used to study shock propagation during crises¹⁷. Additionally, the model provides a thermodynamic construction of networks at the Walrasian economic equilibrium^{56,57}, according to which agents in an exchange economy care only about final allocations and are indifferent with respect to various market configurations (i.e., network structures) that realize the same allocations. Hence, comparison with the null model allows us to assess how far the empirical networks are from their equilibrium configurations induced by the production structure of each firm, and whether significant deviations appear in the presence of exogenous macroeconomic shocks. Figure 1 illustrates our working pipeline.

Our results reveal that at the onset of the COVID-19 pandemic, the composition of firms bearing the highest systemic risk undergoes a fundamental shift, with firms facilitating economic exchanges emerging as central players in the network – a structural transformation that cannot be replicated by the s-GM null model. While systemic risk closely follows null expectations before the pandemic, it diverges significantly afterward, reflecting an adaptive reconfiguration of economic interactions that enhances resilience both in absolute terms and relative to equilibrium predictions. Using regression analysis (see Methods) we find that international trade volume becomes a key predictor of firms' systemic risk dynamics during the crisis, yet global linkages alone cannot fully account for the observed trends. Imports and exports exert opposing influences on local systemic risk through supply and demand mechanisms, underscoring the complexity of risk propagation in globally interconnected economies.

Results

The Hungarian production network

Supplier-customer relations in the Hungarian economy are obtained from firm-level value added tax (VAT) transaction data^{36,58} (see Methods). Since data contain no information on the type of product exchanged, but only the industrial classification of

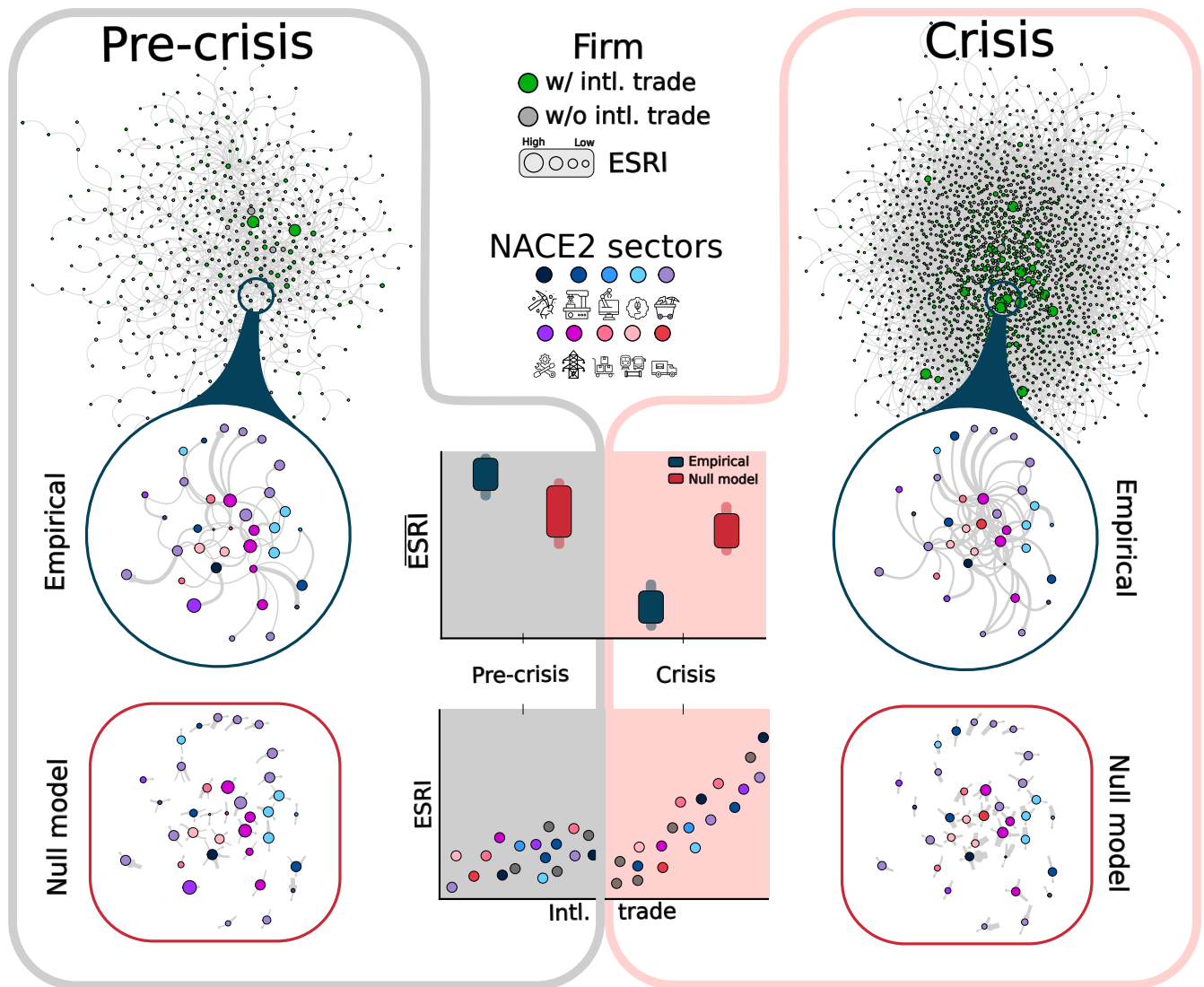


Figure 1. Empirical and null model networks are compared before and during the COVID-19 crisis, to study the evolution of economic systemic risk and understand the role of international trade. We start with temporal snapshots of the empirical production network. The top of the figure shows the network of a sample of the same 1000 nodes, before and during the crisis. Firms are colored according to the presence (green) or absence (gray) of international trade ties, while nodes' size is proportional to firms' ESRI value. We then focus on firms with the highest systemic risk values, highlighted with a circular magnification from the empirical networks, where the nodes' color represents the firms' industrial (NACE2) sector. Finally, the squares in the third row represent the null models for the same set of risky firms, where we show only the constrained quantities (for each firm, its supplies from different sectors and total sales). Our framework thus allows studying the temporal evolution of systemic risk, how it deviates from the predictions of the null model, and which characteristics of the firms, such as the presence of international trade, are linked to their risk value (as shown by the sample analysis plots in the middle of the figure).

firms, we follow the typical assumption in related studies that every firm produces only one out of m different products (goods or services), which is determined by the firm's industry classification. Therefore, we assume that each firm i produces product p_i corresponding to its NACE (Statistical Classification of Economic Activities in the European Community⁵⁹) classification scheme on the 4-digit level, with a total of $m = 615$ product categories.

The data is then represented as a directed weighted network, where nodes correspond to firms and a link from supplier firm i to buyer firm j is established when data report a transaction from j to i , with value $w_{i \rightarrow j}$ corresponding to the volume of product type p_i delivered from i to j . We aggregate transactions between firms on a yearly basis to build production networks for the time range 2015-2022.

These networks are extremely large, with hundreds of thousands of firms and millions of transactions. To make these networks computationally manageable and at the same time to remove possible geographical effects, we only consider firms whose headquarters are based in Budapest (the vast majority of firms in Hungary) and remove very small firms (in terms of employees and customers – see Methods and Supplementary Materials S1 and S2 for further details). In this way, we decrease the size of the network by a factor of ten and obtain yearly snapshots of the *local* production network of Budapest (see Table 2 in Methods).

The number of firms and transactions in the yearly networks grow substantially over time (Figure 2A), with a big jump observed in 2018, which can be attributed to the use of online cash registers imposed by the government in 2017¹ and the introduction of the Real-Time Invoice Reporting (RTIR) for all domestic invoices above 100000 HUF in 2018². Thus from 2018 onward data start to include many small firms, which mainly have few connections (also because of the reporting threshold applied on the data, see Methods), resulting in a drastic drop of the link density of the network. Concerning node-level statistics for each time snapshot, the trading volume of each firm i is described by its out-strength (total sales) $s_i^{\text{out}} = \sum_j w_{i \rightarrow j}$ and in-strength (total purchases) $s_i^{\text{in}} = \sum_j w_{j \rightarrow i}$, whereas, the firm's connectivity is described by its out-degree (number of customers) $k_i^{\text{out}} = \sum_j a_{i \rightarrow j}$ and in-degree (number of suppliers) $k_i^{\text{in}} = \sum_j a_{j \rightarrow i}$, where $a_{i \rightarrow j} = 1$ if $w_{i \rightarrow j} > 0$ (and 0 otherwise). Similarly to previous research in other production networks²⁷, we find power-law tails (without cut-off⁶⁰) in the distribution of these quantities (Figure 2 B-C-E-F), and that the total sales / number of customers is typically much larger than the total supply / number of suppliers, respectively. The tails of the distributions grow in time due to the increasing presence of large firms in the network; however, while the strength distributions are rather stable, degree distributions progressively shift to higher values.

Evolution of Economic Systemic Risk of firms

To assess how firm-level systemic risk evolves throughout the years, we compute the *Economic Systemic Risk Index* (ESRI)³⁶ of all firms in each yearly network. In a nutshell, the systemic risk of a firm is computed by removing it from the network and iteratively propagating the upstream (demand) and downstream (supply) shock to connected firms in the production network, which respectively occur when a customer stops buying a product and when a supplier stops selling a product. The ESRI of the firm then corresponds to the overall output reduction of the network due to its failure (see Methods for more details on the ESRI computation, and Supplementary Materials S3 and S4 for how ESRI relates to the firm's degree and strength values).

We first consider the time series of average and total ESRI values of all firms for each year (Figure 2D). The decreasing trend of the average ESRI is tied to the decreasing network density, which implies relatively less connections and thus fewer shock propagation channels. On the other hand, the growing trend of the total ESRI sum mirrors the growth in number of nodes of the yearly networks. We then focus on the evolution of single-firm ESRI values, to understand whether they are stable or vary over years (despite firms frequently rewire their connections⁶¹). By computing the Pearson correlation coefficient of firm-level values for each pair of years, we find strong consistency of ESRI over time (Figure 2G), even when the network structure changes considerably from year 2017 to 2018. However, the drop in correlation observed from 2019 to 2020 suggests that COVID brought about deep network changes that influenced firms' potential impact on the economy (for further insights into yearly ESRI correlations for upstream and downstream values separately, refer to Supplementary Materials S5).

As highlighted in previous research^{36,55}, plotting ESRI values versus ESRI rankings reveals a plateau composed of the most risky firms, followed by a steep decrease for higher rankings (shown in Figure 2H for 2015 and in Figure 2I for 2021, see Supplementary Materials S6 for the other years). Plateau firms represent the biggest threat to the network: according to ESRI, their failure would result in the loss of about 10 to 15% of the total output of the local Budapest economy.

We observe that the shape of the plateau, together with the downstream and upstream values, remains consistent in time until 2019, while starting from 2020 the upstream ESRI shows large positive variations that are responsible for the emergence of a step-like structure of the plateau. In particular, the growth in upstream ESRI scores for the plateau firms can be associated with an increase in the firms' in-strength (see previous analysis), which can be attributed to firms increasing their connections with local firms to replace those with foreign countries, restricted due to COVID.

Empirical vs null model values of ESRI

To benchmark empirical values of ESRI to a null model, using the s-GM method we construct an ensemble of 100 networks for each year in our data (see Methods for the s-GM description, and Supplementary Materials S7 where we show that the model is able to reproduce the degree and strength statistics of the empirical network). We compute the ESRI values of all firms for each of these networks and then average over the ensemble to obtain null yearly values of ESRI for each firm.

Similarly to the empirical network, ESRI values in the null model are stable across subsequent years, as revealed by high Pearson correlation coefficients (Figure 3A). However, while for empirical values the highest change is observed between 2019

¹<https://www.vatcalc.com/hungary/hungary-online-real-time-vat-cash-registers/>

²https://www.storecove.com/blog/en/e-invoicing-in-hungary/?unbounce_brid=1699967181_5491104_e17e0a18c82a49f0b68fce7880aba2eb

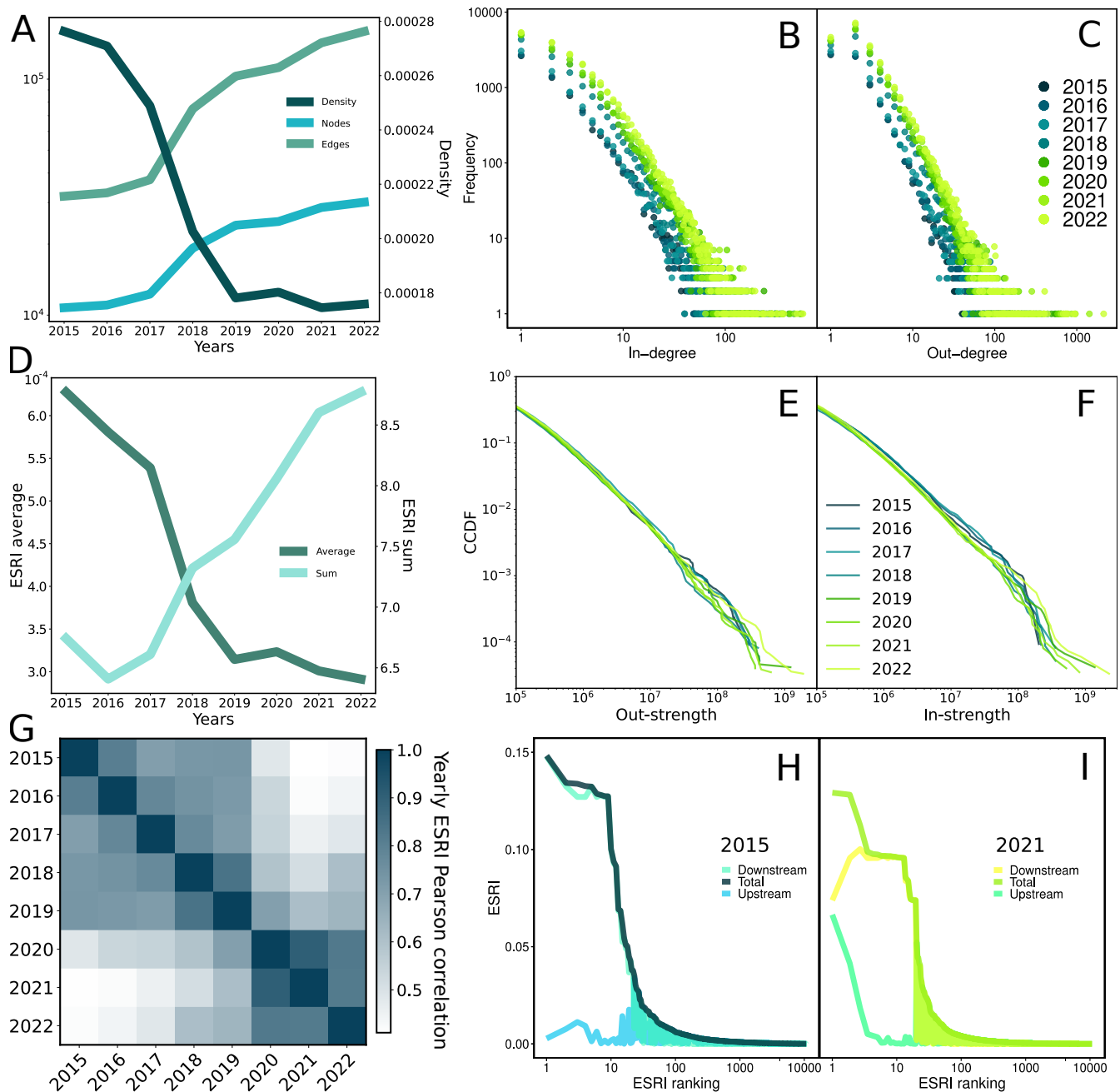


Figure 2. Time evolution of topological properties and systemic risk of the empirical production networks. A) Number of nodes (firms), links (transactions) and density of the local Budapest production network in the considered time range. B) Probability distributions of out-degree (number of customers per firm) for all yearly production networks. C) Probability distribution of in-degree (number of suppliers) for all yearly production networks. D) Average and total ESRI of firms in the yearly networks. E) Tail of the survival distribution of out-strength values (total sales of firms) of yearly production networks. F) Tail of the survival distribution of in-strength values (total supply of firms) of yearly production networks. G) Matrix of Pearson correlation coefficients for ESRI values of firms among different years. H) ESRI values vs rankings for the total, upstream and downstream components for 2015. I) ESRI values vs rankings for the total, upstream and downstream components for 2021.

and 2020 (the onset of COVID), for the null model changes are more pronounced in going from 2017 to 2018, when the real network experienced a considerable growth in nodes and links. This result suggests that the null model is not able to fully capture the underlying dynamics of ESRI evolution in time when the system is affected by exogenous shocks. Nonetheless,

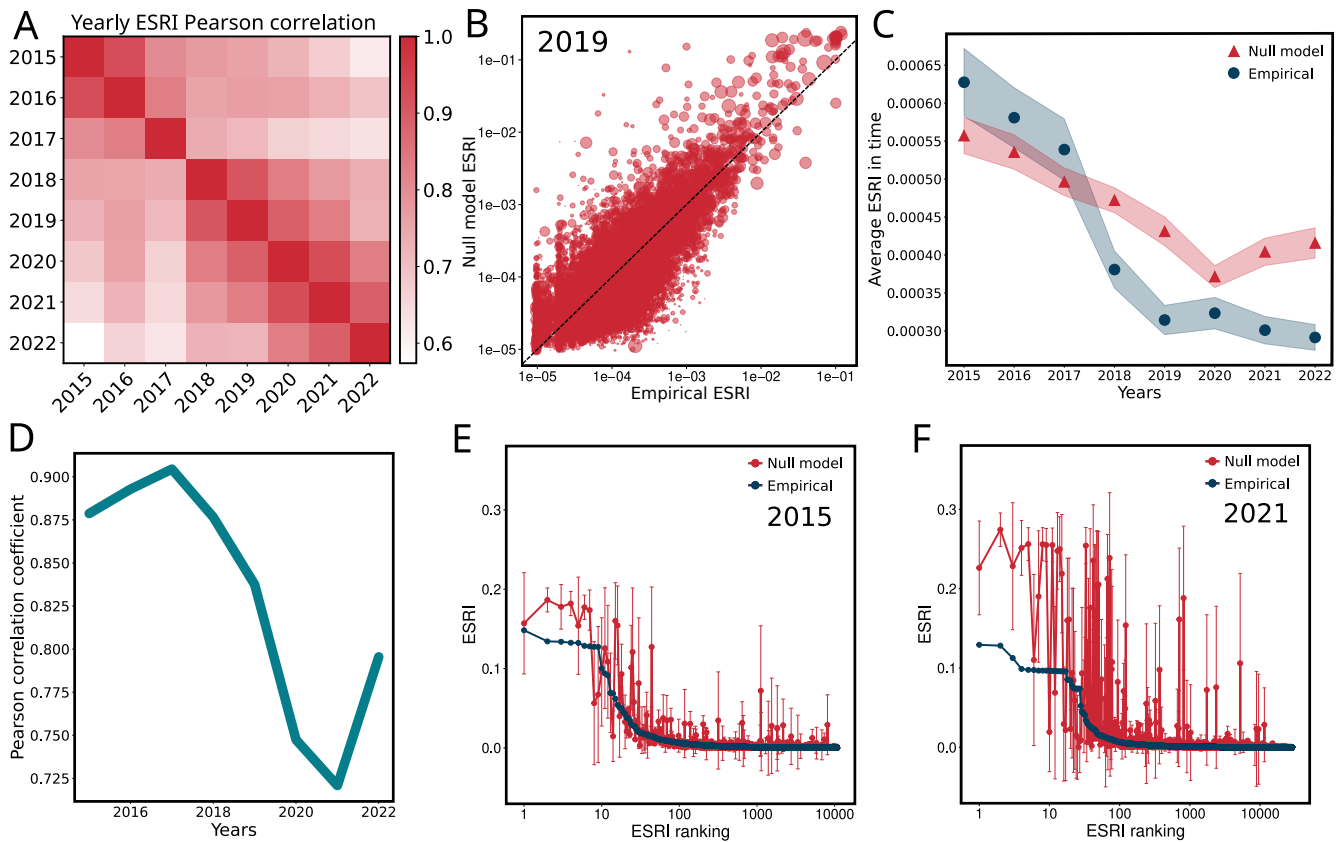


Figure 3. Empirical vs null model ESRI values. A) Matrix of Pearson correlation coefficients for null ESRI values of firms among different years. B) Empirical vs null ESRI values of individual firms for 2019. The size of each point corresponds to the firm’s number of employees, here taken as proxy for size. C) Mean value of ESRI for empirical and null networks. Shaded area refers to standard deviations (which are larger for the model due to the sampling procedure). D) Pearson correlation coefficient of empirical vs null ESRI values of individual firms, for each year. E) Empirical and null ESRI ranking for year 2015. F) Empirical vs null ESRI ranking for year 2021. Error bars represent standard deviations among ensemble values. Model values are ordered according to their empirical ranking.

as shown in Figure 3B for year 2019 (see Supplementary Materials S8 for the other years), there is a very good agreement between real and model ESRI values for individual firms for each of the yearly networks, as most of the points lie along the identity line. Some discrepancies arise as the model slightly overestimates ESRI of the most risky firms (top right corner), while underestimating that of the least risky ones (bottom left corner). This is mainly due to the sampling method at the basis of the s-GM, for which small firms may happen to get disconnected from the network in some model samples⁶². These firms then have very small ESRI, as they cannot propagate shocks to others. At the same time, since the link density is preserved, bigger firms may then receive slightly more connections, increasing their impact with respect to the empirical case. Considering global statistics, the average values of the empirical and null model ESRI across all firms are statistically compatible from 2015 to 2017 (Figure 3C). However, from 2018 onward, the model ESRI becomes significantly higher than the real one, possibly because the small firms entering the network in this period follow different market dynamics that are not captured by the null model. Notably the deviation increases in 2020-2022, when we witness opposite trends of empirical and null values. Furthermore, the Pearson correlation coefficient between real and model ESRI scores drops in 2020-2021, during the flare-up of COVID (Figure 3D). These results suggest that the null model, which works well both in reconstructing the empirical networks⁵⁴ and reproducing the ESRI dynamics⁵⁵ during normal times, becomes unable to faithfully do so during times of crisis, as the real networks deviate from their equilibrium configurations. This deviation may be the result of additional network formation mechanisms at work during that period – which are not included in the null hypothesis underlying the s-GM.

To further corroborate this statement, we compare empirical and model rankings of ESRI for individual firms (Figure 3E-F). The overestimation of null ESRI for highly risky firms, discussed above, leads to a higher plateau for model values. Overall we observe a good agreement between the empirical and model curves for 2015, with deviations between 0.05 and 0.1 only for a handful of ten firms and much lower for the others, confirming that, in normal times, the s-GM provides accurate

estimates of single-firm ESRI values⁵⁵. However, this is not the case for 2021, as the model rankings become more disordered and unable to correctly reproduce not only the plateau, but most of the ranking as well. Indeed we observe deviations above 0.05 (and up to 0.2) for about 40 firms. The mismatch between empirical and model values grows steadily starting from 2018, with 2021 and 2022 yielding the largest deviations (refer to Supplementary Materials S9 for ranking plots of all years, to Supplementary Materials S10 for plots of the deviations between real and null model values, and to Supplementary Materials S11 for distributions of empirical and null model ESRI values).

Sector composition of ESRI plateaux

We now focus on the most risky firms, namely those that belong to the ESRI ranking plateaux. For each year, we select plateau firms as the top 0.1% of the corresponding ESRI ranking (see Supplementary Materials S12 for the full list of NACE4 sectors of these companies). Figure 4A provides a graphical illustration of the time evolution of the empirical network composed of only the plateau firms, colored by NACE2 sector and sized according to their ESRI values. The set of plateau firms changes throughout the years (Figure 4B), with a Jaccard index between consecutive years of about 0.5 in ordinary times (meaning that about half of the firms remain in the plateau from one year to the next one) and of 0.7 for the COVID years 2020-2022 (pointing to a rather stable composition of the plateaux).

Among the top firms, a few remain in the plateau for the entire period analyzed. They correspond to NACE2 code 35 (electricity, gas, steam and air conditioning supply) and 28 (manufacture of machinery and equipment). In addition, all plateau firms belong to only a handful of industrial sectors (see Supplementary Materials S13 for more details).

We then compare the plateau composition in empirical and null model networks of the same year, where model plateau firms are selected using the corresponding null ESRI rankings. The overlap between the sets of firms in the empirical and model plateaux is high in most years, but decreases noticeably during the pandemic (Figure 4C), when the null model cannot identify all of the most risky firms: In line with the previous result, the model becomes less compatible with the empirical network during COVID-19. To better analyze the time evolution of the sector composition of the plateau we focus on a stable set of top firms, as those that appear in the empirical plateaux for more than three years. Figure 4D shows the temporal evolution of ESRI for all these firms, summed over NACE2 sectors, for both empirical and null model networks.

Concerning empirical values, we observe a decreasing trend of ESRI for the majority of these sectors, while there is a steep increase in ESRI for the postal activity sector, which represents an emblematic example of the impact of COVID on the production network: due to mobility restrictions, postal services became crucial for the entire system, by allowing trade transactions and maintaining the economy running⁶³. The ESRI values for the null model, instead, grow steadily in time, including during COVID years.

We may argue this occurs because the null model is simply driven by the increase in degrees and strengths of the largest firms in the empirical networks during the years (see the increasing tail in the distributions of Figures 2 B-C-E-F), which results in more interconnections and thus higher systemic-ness for these firms. The growth of these statistics could be partly caused by import bans that forced companies to search for products in the domestic economy, thus increasing the connections and exchanges we see in the data. Since the s-GM directly constrains the strength values, it is already taking into account this increase in local trade, therefore null model ESRI values of large firms become higher during COVID. On the other hand, in the empirical case, the increase in connections and strengths does not result in an ESRI increase for large firms which, apart from the postal services, display a decreasing trend. In fact, while the postal services represented the only available alternative to bypass lockdown measures, resulting inevitably in an increase of its ESRI value, other firms could decide how to eventually rewire their links (for example to cope with import bans). Notably, this optimization process at the level of individual firms also led to a more resilient network configuration at the global level. Of course, these mechanisms at work during times of crises are not captured by the null model.

Determinants of firm-level systemic risk

To understand the drivers of firm-level systemic risk in the local production network, we estimate the ESRI value of firms in each year t using a multivariate regression, in which explanatory variables include the systemic risk indicator of the s-GM null model ($ESRI_{model}$). Adding further company characteristics to the regression allows us to explain the variance in empirical ESRI that null model ESRI cannot describe. The latter contain features that might be important for ESRI calculation, such as firm size measured by number of employees (*Employment*), its importance in the local trade network measured by in-strength and out-strength of trade flows (*Strength_{in}*, *Strength_{out}*) and *Essentiality* – the fraction of customers for which the firm's input is essential, computed according to the essentiality matrix of¹⁷. In addition, we include volume of international trade (*Import*, *Export*) that can be non-trivially related to systemic risk in the local economy by generating spillovers from international product flows through local links in the production network. The regression includes company fixed-effects that capture further unobserved firm characteristics and year dummies that control for yearly fluctuations (see Methods for a more detailed presentation of the regression model and the variables included, and Supplementary Materials S14 for the correlation table of firm features).

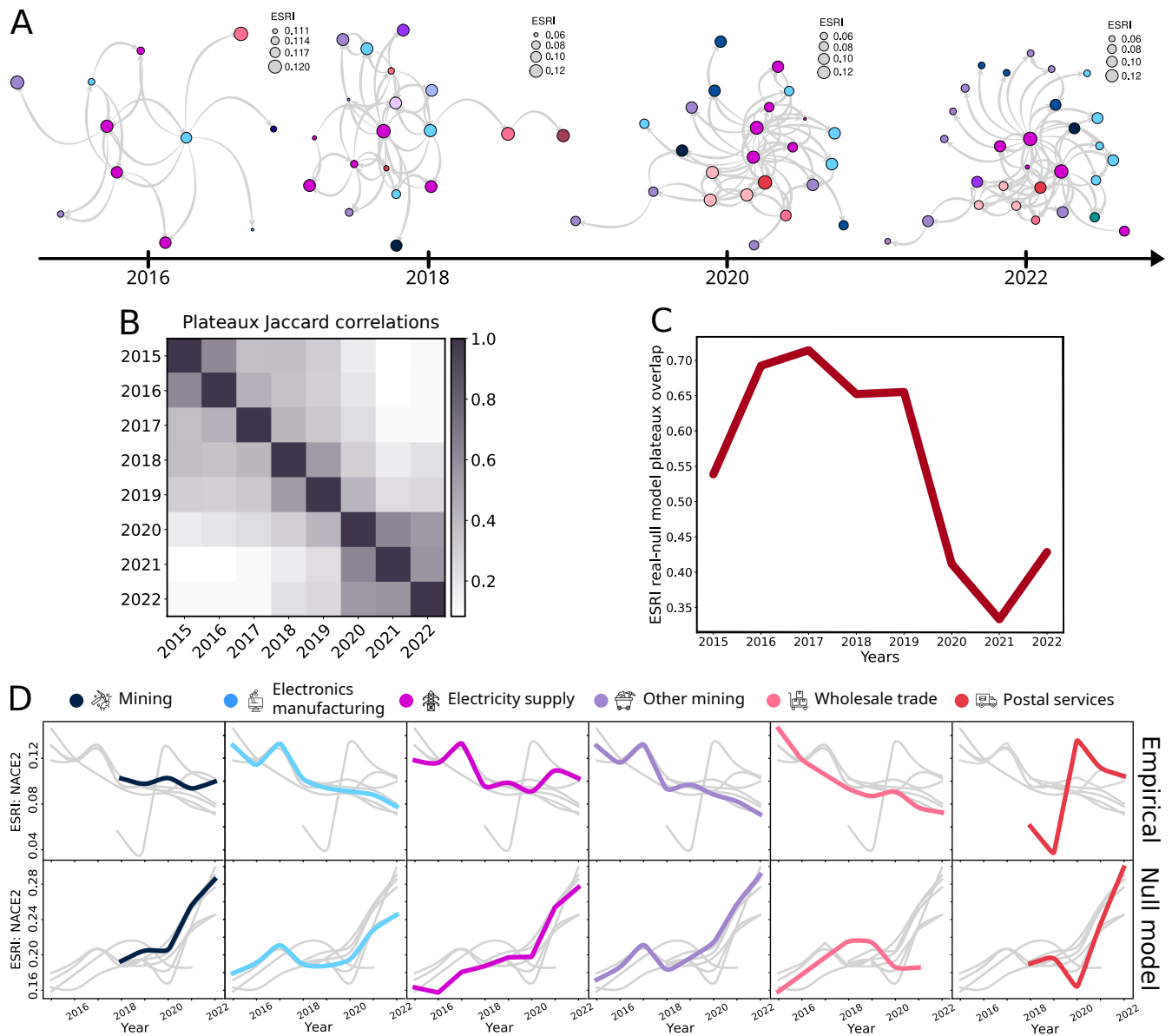


Figure 4. ESRI plateaux analysis. A) Representation of the empirical network among plateau firms, with node size proportional to ESRI values and color identifying the NACE2 sector. B) Matrix of Jaccard indices quantifying the overlap among the sets of empirical plateaux firms between different years. C) Time evolution of the Jaccard coefficient of plateau firms sets between empirical vs model networks in the same year. D) Evolution of empirical (top panels) and null (bottom panels) ESRI values, for firms appearing more than 3 years in the plateaux, grouped by NACE2 sectors. Each panel highlights the evolution of a single sector (the other sectors are displayed in gray).

In Table 1 we present a series of regressions, in which models including either *Import* (Models 1-4) or *Export* (Models 5-8) are separated due to the high correlation of these variables. Regressions (1) and (5) allow to understand the influence each variable has on the value of the empirical ESRI for a given firm. As expected, we find a strong correlation between empirical ESRI and null model values. Growing intensity of local trade is associated with increasing ESRI, especially if the company's supply is essential for the customers' businesses. Size effects are stronger for out-strength than in-strength, because the former is related to downstream shocks, which propagate with a generalized Leontief production function, while upstream shocks propagate linearly. *Essentiality* has a strong positive correlation with *ESRI*, signaling that systemic risk is higher for those firms that provide essential inputs for many other firms in the local economy. Overall, the contributions of these variables containing information of the local trade network are in line with expectations and also seem to capture the scale effects, since

Employment has no significant relationship with ESRI (not reported in 1).

The positive and significant coefficients of *Import* (1) and *Export* (5) signal that international trade can also increase systemic risk of companies in national economies. This result is non-trivial, but paired with local links, increasing international trade can ripple through to local economic systems. To disentangle these mechanisms, we add the interaction terms between international trade and local trade variables and find that the impact of international trade on local systemic risk through domestic links (represented by in- and out-strengths) shows a mixed picture. On the one hand, the negative interaction term in (2) between *Import* and *Strength_{out}* as well as *Essentiality* signals that import does not have a spillover impact on systemic risk in the local economy of Budapest. Due to the dominance of multinational companies in manufacturing sectors that are more embedded in global value chains than in local economies^{64,65}, importing companies probably sell their products predominantly on export markets, instead of distributing imported goods through local links. As a result, we see a negative association of *Import* × *Strength_{out}* with *ESRI*. However, the positive interaction term between *Import* and *Strength_{in}* in Models (3) and (4) signals that firms can also complement domestic supplies and thus increase the firm-level *ESRI* altogether. On the other hand, the interaction of *Export* with *Strength_{out}* and *Essentiality* is negatively correlated with *ESRI* (6), suggesting that increasing exports can decrease systemic risk in the domestic economy, in case they substitute local revenues. However, increasing export is associated with increasing *ESRI* of companies if their production demands more input links locally.

Splitting the period into pre-COVID years (3,7) and COVID years (4,8) reveals that both *Import* and *Export* become significantly correlated with *ESRI* only during COVID. This can be explained considering that during COVID there was an

Table 1. Fixed-effects panel regressions with empirical *ESRI* as the dependent variable. Given the high correlation between *Import* and *Export*, the two variables have been taken into consideration separately. Unreported control variables include *Employment*. ***, **, * denote significance at the 1%, 5%, 10% level. Standard errors in parentheses.

| | ESRI | | | | | | | |
|---|---------------------|----------------------|----------------------|----------------------|---------------------|----------------------|----------------------|----------------------|
| | (1) | (2) | (3) | (4) | (5) | (6) | (7) | (8) |
| | | | (2015- 2019) | (2020- 2022) | | | (2015- 2019) | (2020- 2022) |
| <i>ESRI_{model}</i> | 0.319*** (0.004) | 0.319*** (0.004) | 0.287*** (0.007) | 0.243*** (0.007) | 0.319*** (0.004) | 0.317*** (0.004) | 0.285*** (0.007) | 0.243*** (0.007) |
| <i>Import</i> | 0.003*** (0.000) | 0.008*** (0.002) | 0.005 (0.003) | 0.020*** (0.004) | | | | |
| <i>Export</i> | | | | | 0.003*** (0.001) | 0.006* (0.003) | -0.002 (0.004) | 0.021*** (0.006) |
| <i>Strength_{out}</i> | 0.058*** (0.003) | 0.060*** (0.003) | 0.063*** (0.005) | 0.103*** (0.006) | 0.058*** (0.003) | 0.060*** (0.003) | 0.062*** (0.005) | 0.102*** (0.006) |
| <i>Strength_{in}</i> | 0.039*** (0.001) | 0.038*** (0.001) | 0.041*** (0.001) | 0.032*** (0.001) | 0.039*** (0.001) | 0.038*** (0.001) | 0.040*** (0.001) | 0.032*** (0.001) |
| <i>Essentiality</i> | 0.470*** (0.005) | 0.480*** (0.005) | 0.480*** (0.009) | 0.491*** (0.009) | 0.470*** (0.005) | 0.474*** (0.005) | 0.480*** (0.008) | 0.480*** (0.008) |
| <i>Import</i> × <i>Strength_{out}</i> | | -0.001*** (0.001) | -0.001 (0.001) | -0.004*** (0.001) | | | | |
| <i>Import</i> × <i>Strength_{in}</i> | | -0.000 (0.000) | 0.001*** (0.000) | 0.001*** (0.000) | | | | |
| <i>Import</i> × <i>Essentiality</i> | | -0.004*** (0.001) | -0.003*** (0.002) | -0.004*** (0.002) | | | | |
| <i>Export</i> × <i>Strength_{out}</i> | | | | | | -0.002*** (0.001) | 0.000 (0.001) | -0.006*** (0.001) |
| <i>Export</i> × <i>Strength_{in}</i> | | | | | | 0.002*** (0.000) | 0.001*** (0.000) | 0.002*** (0.001) |
| <i>Export</i> × <i>Essentiality</i> | | | | | | -0.004*** (0.001) | -0.007*** (0.002) | 0.002 (0.002) |
| N | 137956 | 137956 | 65639 | 72317 | 137956 | 137956 | 65639 | 72317 |
| R ² | 0.388 | 0.389 | 0.357 | 0.310 | 0.388 | 0.389 | 0.357 | 0.310 |
| F Statistic | 4399.917*** | 3579.652*** | 1517.326*** | 1472.027*** | 4398.629*** | 3580.783*** | 1518.955*** | 1469.652*** |

overall drop in trade due to import and export difficulties all over the globe. Thus, only the largest and truly essential firms were allowed to maintain trade with foreign countries, and these firms get the highest ESRI values (see Supplementary Materials S15 for a correlation of ESRI, essentiality and size, proxied by the firm's out-strength).

Consequently, the above reported impact of import on national systemic risk through local production networks is only apparent during the COVID period in our case (4). However, we find that the effect of export is slightly different with respect to COVID. While exports as supplements for domestic revenues only decrease ESRI during COVID, they only substitute essential links in the pre-COVID period. We find a stable positive and significant joint effect between *Export* and *Strength_{in}* in both pre- and COVID years. This signals that increasing export may increase systemic risk in national production networks if it increases the demand for local inputs.

We run a series of robustness checks that provide further support for the above results. Pooled OLS regressions with year fixed-effects and cross-sectional linear regressions run by years are reported in Supplementary Materials S16, S17 and S18.

Conclusions

Studying how systemic risk of individual firms evolves in time and changes due to external shocks is of fundamental importance when studying economic networks, as it discloses many of the mechanisms responsible for shock propagation throughout supply and demand links. In this work we analyzed, for the first time, the evolution of the Economic Systemic Risk Index³⁶ for all firms belonging to the VAT transaction network of Budapest from 2015 to 2022. We compared the results found for the empirical networks with expectations from the stripe-corrected gravity model⁵⁴, a maximum-entropy framework that constrains the input by sector and output flow of each firm in the economy. Our findings highlight a consistent correlation between ESRI values throughout the years, with a visible disruption in the COVID years 2020–2022, when systemic risk decreases both in absolute terms and with respect to the equilibrium values of the null model. Our interpretation of this finding is that, to cope with the shock induced by the pandemic, the forced closure of many companies and the limits to the import/export of goods, firms rewired their connections and thus diminished their systemic risk⁶⁶. In fact, while all firms with highest risk display a decreasing trend in time, only the postal sector shows an opposite behavior, as this service becomes essential in maintaining connections between different firms, thus preserving economic exchanges. The regression analysis allowed to shed light on how different firm variables are linked to systemic risk, highlighting that local trade and export are strongly correlated with ESRI, while import seems to have a spillover effect only during COVID years. Overall, this work paves the way to a temporal analysis of systemic risk and shock propagation on economic networks, disclosing how firms change their suppliers and rewire their connections to deal with wavering conditions.

One of the limitations of our work is the computational cost of ESRI calculation, which made us focus on the local Budapest network rather than the whole network of Hungary, and considerably limited the size of the null model ensemble we were able to handle.

Future work will focus not only on the impact of firms failure on the economy, as measured by ESRI, but also on their resilience – namely the ability to cope with supply and demand shocks. Additionally, by using data on firm's location and mobility we could be able to determine which firms were affected more by COVID restrictions, and how it relates to their economic resilience.

Methods

Data description and filtering

The Hungarian production network is obtained from VAT transaction data as follows. For every sales transaction between a supplier i and buyer j , we have the monetary value of the goods and services sold, V_{ji} in forints (HUF), and the tax amount paid T_{ji} . We use V_{ji} as an estimate for the volume w_{ij} of product type p_i delivered from i to j . We aggregate all transactions on a yearly basis by summing all exchanges between two firms that take place in a given year.

Transactions for years 2015 to 2017 appear in the dataset only if they exceed a reporting VAT threshold of $t = 1\,000\,000$ HUF (about 2500 EUR). In order to make the whole dataset homogeneous we apply the same threshold for all other years, thus removing transactions with value less than t . We also implement two additional filters. To build a local production network and remove possible geographical effects or biases, we only consider firms whose headquarters are based in Budapest (which are the majority of firms in Hungary). Furthermore, in order to make the yearly networks easier to handle, for each snapshot we also remove small firms that have a number of employees ≤ 11 and also a number of customers $k^{\text{out}} \leq 2$. See Supplementary Materials S1 and S2 for further information on the goodness of the filters.

The Economic Systemic Risk Index

The *Economic Systemic Risk Index* (ESRI) quantifies the systemicness of a firm by evaluating the output reduction experienced by the whole production network due to its failure. More in detail, the removal of firm i from the network (meaning that it

| Year | Pre-filtering | | Post-filtering | |
|------|---------------|--------------|----------------|--------------|
| | Firms | Transactions | Firms | Transactions |
| 2015 | 88992 | 221200 | 10745 | 31893 |
| 2016 | 93258 | 225165 | 11032 | 32967 |
| 2017 | 101590 | 25494 | 12267 | 37456 |
| 2018 | 272410 | 1373207 | 19224 | 74866 |
| 2019 | 305492 | 2059287 | 24039 | 102928 |
| 2020 | 440715 | 12457336 | 24921 | 111953 |
| 2021 | 448750 | 18147540 | 28580 | 159308 |
| 2022 | 457239 | 19050904 | 30098 | 159308 |

Table 2. Number of firms and transactions for all yearly networks, before and after the filtering procedure.

stops buying from its suppliers and supplying to its customers) generates an upstream and a downstream shock. The shocks are propagated to all other firms $j \neq i$ by recursively updating their production levels. The fraction of original production firm j can maintain at iteration n after having received the shocks is defined as $h_j^d(n)$ for the downstream shocks and $h_j^u(n)$ for the upstream ones. The downstream shock propagates according to a generalized Leontief *production function*²⁵. Inputs from *essential* sectors set a Leontief-kind of constraint on the output of firms, while the inputs from *non-essential* sectors are treated in a linear way. The identification of essential products, according to their NACE4 industry classification, is provided by expert based surveys^{17,67}, while the technical coefficients of the production function are calibrated on the empirical network. The shock propagation dynamics is iterated until iteration n^* , when a stable state is reached that satisfies a given convergence threshold. The final production level of every firm is then set as $h_j(n^*) = \min[h_j^d(n^*), h_j^u(n^*)]$. Finally, the ESRI of firm i is computed by summing the output reduction of each firm in the network

$$ESRI_i = \sum_{j=1} \frac{s_j^{out}}{\sum_{l=1} s_l^{out}} [1 - h_j(n^*)] \quad (1)$$

We remand the reader to³⁶ for full details of the method.

The Stripe-Corrected Gravity Model

Unbiased null models of networks can be defined within the framework of Exponential Random Graphs (ERGs)^{47,48}. For this approach to work in the context of heterogeneous weighted complex networks that are sparse (as is the case of production networks), the typical recipe is to constrain node strengths (the total weight of incident connections) as well as node degrees (the number of connections per node)^{68,69}. This can be done using a heuristic two-step procedure, known as *density-corrected gravity model* (d-GM), assessing first whether two nodes are connected and then the value of the link weights^{70,71}. The first step is based on the canonical *configuration model*⁷² where model parameters controlling the degrees are replaced by node strengths using a *fitness ansatz*^{73,74}. The *stripe-corrected Gravity Model* (s-GM)⁵⁴ improves the d-GM recipe by constraining the sector-specific strength of each node (rather than the overall strength), preserving in this way the input-output productive structure of each firm. Specifically the model preserves, for each firm j , the total output $s_j^{out} = \sum_i w_{j \rightarrow i}$ as well as the list of input quantities by industry g , namely $s_{g \rightarrow j} = \sum_{i \in g} w_{i \rightarrow j}$, which is a good proxy for the amount of products by industry that the firm uses to produce its output. The model follows a two-step procedure that first estimates the probability of a connection from supplier i to customer j :

$$p_{i \rightarrow j} = \frac{z_{g_i} s_i^{out} s_{g_i \rightarrow j}}{1 + z_{g_i} s_i^{out} s_{g_i \rightarrow j}}, \quad \forall i \neq j \quad (2)$$

where g_i is the industrial sector of the supplier i , and then assigns the link weight according to:

$$w_{i \rightarrow j} = \frac{s_i^{out} s_{g_i \rightarrow j}}{w_{g_i}^{tot} p_{i \rightarrow j}}, \quad \forall i \neq j \quad (3)$$

where $w_{g_i}^{tot} = \sum_{k \in g_i} \sum_j w_{k \rightarrow j} = \sum_{k \in g_i} s_k^{out} = \sum_j s_{g_i \rightarrow j}$ is the total outgoing strength of sector g_i . We employ the multi-z variant of the s-GM, thus we have a different parameter z_{g_i} for each industrial sector, which can be determined by solving the equations $\sum_{k \in g_i} \sum_{j \neq k} p_{k \rightarrow j} = L_{g_i}$ where $L_{g_i} = \sum_{k \in g_i} \sum_j a_{k \rightarrow j}$ is the number of outgoing links from sector g_i . By construction the model

preserves, on average, the total out-strength and the in-strength by sector of each firm, thus reproducing the production structure of the empirical network:

$$\langle s_i^{out} \rangle = \sum_j \langle w_{i \rightarrow j} \rangle = s_i^{out} \frac{\sum_j s_{g_i \rightarrow j}}{w_{g_i}^{tot}} = s_i^{out}, \quad \forall i, \quad \langle s_{g_i \rightarrow j} \rangle = \sum_{k \in g_i} \langle w_{k \rightarrow j} \rangle = s_{g_i \rightarrow j} \frac{\sum_{k \in g_i} s_k^{out}}{w_{g_i}^{tot}} = s_{g_i \rightarrow j}, \quad \forall j, g_i \quad (4)$$

Regression framework

To analyze the dynamics of firms' systemic risk, we estimate *ESRI* values of company *j* at year *t* in a multivariate fixed-effect panel regression, following the formula:

$$ESRI_{j,t} = \alpha + \beta_1(ESRI_{model})_{j,t} + \beta_2 E_{j,t} + \beta_3 LT_{j,t} + \beta_4 IT_{j,t} + \beta_5(LT_{j,t} \times IT_{j,t}) + \mu_j + \varepsilon_{j,t}, \quad (5)$$

where *ESRI_{model}* denotes the average of ESRI values from the null model, *E_j* stands for company size (number of employees), *LT_j* is the characteristics of local trade measured in the production network (out-strength, in-strength, essentiality score), *IT_j* denotes the value of international trade (import and export), *μ_j* is the company fixed-effect and *ε* is the error term. This framework allows for assessing the determinants that can explain firms' systemic risk, beyond the null model expectations. The interaction term between *LT* and *IT* enables us investigate how international trade is related to local systemic risk, mediated by local trade channels.

References

- Atalay, E., Hortaçsu, A., Roberts, J. & Syverson, C. Network structure of production. *Proc. Natl. Acad. Sci.* **108**, 5199–5202, DOI: <https://doi.org/10.1073/pnas.1015564108> (2011).
- Lőrincz, L., Juhász, S. & O. Szabó, R. Business transactions and ownership ties between firms. *Netw. Sci.* **12**, 1–20, DOI: [DOI:10.1017/nws.2023.19](https://doi.org/10.1017/nws.2023.19) (2024).
- McNerney, J., Savoie, C., Caravelli, F., Carvalho, V. M. & Farmer, J. D. How production networks amplify economic growth. *Proc. Natl. Acad. Sci.* **119**, e2106031118, DOI: [10.1073/pnas.2106031118](https://doi.org/10.1073/pnas.2106031118) (2022).
- Zoltán Elekes, R. B. & Lengyel, B. Foreign-owned firms as agents of structural change in regions. *Reg. Stud.* **53**, 1603–1613, DOI: [10.1080/00343404.2019.1596254](https://doi.org/10.1080/00343404.2019.1596254) (2019). <https://doi.org/10.1080/00343404.2019.1596254>.
- Choi, T. Y. & Krause, D. R. The supply base and its complexity: Implications for transaction costs, risks, responsiveness, and innovation. *J. operations management* **24**, 637–652, DOI: <https://doi.org/10.1016/j.jom.2005.07.002> (2006).
- Craighead, C. W., Blackhurst, J., Rungtusanatham, M. J. & Handfield, R. B. The severity of supply chain disruptions: Design characteristics and mitigation capabilities. *Decis. Sci.* **38**, 131–156, DOI: <https://doi.org/10.1111/j.1540-5915.2007.00151.x> (2007).
- Cheng, C.-Y., Chen, T.-L. & Chen, Y.-Y. An analysis of the structural complexity of supply chain networks. *Appl. Math. Model.* **38**, 2328–2344, DOI: <https://doi.org/10.1016/j.apm.2013.10.016> (2014).
- Amit Surana, M. G., Soundar Kumara & Raghavan, U. N. Supply-chain networks: a complex adaptive systems perspective. *Int. J. Prod. Res.* **43**, 4235–4265, DOI: [10.1080/00207540500142274](https://doi.org/10.1080/00207540500142274) (2005).
- Vokurka, R. J. & Lummus, R. R. The role of just-in-time in supply chain management. *The Int. J. Logist. Manag.* **11**, 89–98, DOI: [10.1108/09574090010806092](https://doi.org/10.1108/09574090010806092) (2000).
- Barrot, J.-N. & Sauvagnat, J. Input specificity and the propagation of idiosyncratic shocks in production networks. *The Q. J. Econ.* **131**, 1543–1592 (2016).
- Inoue, H. & Todo, Y. Firm-level propagation of shocks through supply-chain networks. *Nat. Sustain.* **2**, 841–847, DOI: <https://doi.org/10.1038/s41893-019-0351-x> (2019).
- Aldrighetti, R., Battini, D., Ivanov, D. & Zennaro, I. Costs of resilience and disruptions in supply chain network design models: A review and future research directions. *Int. J. Prod. Econ.* **235**, 108103, DOI: <https://doi.org/10.1016/j.ijpe.2021.108103> (2021).
- Carvalho, V. M., Nirei, M., Saito, Y. U. & Tahbaz-Salehi, A. Supply chain disruptions: Evidence from the Great East Japan Earthquake. *The Q. J. Econ.* **136**, 1255–1321, DOI: <https://doi.org/10.1093/qje/qjaa044> (2021).
- Rose, A., Chen, Z. & Wei, D. The economic impacts of russia–ukraine war export disruptions of grain commodities. *Appl. Econ. Perspectives Policy* **45**, 645–665, DOI: <https://doi.org/10.1002/aep.13351> (2023). <https://onlinelibrary.wiley.com/doi/pdf/10.1002/aep.13351>.

15. Guan, D. *et al.* Global supply-chain effects of covid-19 control measures. *Nat. Hum. Behav.* **4**, 577–587, DOI: <https://doi.org/10.1038/s41562-020-0896-8> (2020).
16. Chowdhury, P., Paul, S. K., Kaisar, S. & Moktadir, M. A. Covid-19 pandemic related supply chain studies: A systematic review. *Transp. Res. Part E: Logist. Transp. Rev.* **148**, 102271, DOI: <https://doi.org/10.1016/j.tre.2021.102271> (2021).
17. Pichler, A., Pangallo, M., del Rio-Chanona, R. M., Lafond, F. & Farmer, J. D. Production networks and epidemic spreading: How to restart the UK economy? *arXiv preprint arXiv:2005.10585* DOI: <https://doi.org/10.48550/arXiv.2005.10585> (2020).
18. Pichler, A. & Farmer, J. D. Simultaneous supply and demand constraints in input–output networks: the case of covid-19 in Germany, Italy, and Spain. *Econ. Syst. Res.* **34**, 273–293, DOI: <https://doi.org/10.1080/09535314.2021.1926934> (2022).
19. Ivanov, D., Tsipoulanidis, A. & Schönberger, J. *Supply Chain Risk Management and Resilience*, 485–520 (Springer International Publishing, Cham, 2021).
20. Leontief, W. *Input-output economics* (Oxford University Press, 1986).
21. Miller, R. E. & Blair, P. D. *Input-output analysis: foundations and extensions* (Cambridge university press, 2009).
22. Lee, D. Transmission of Domestic and External Shocks through Input-Output Network: Evidence from Korean Industries. IMF Working Papers 2019/117, International Monetary Fund (2019).
23. Contreras, M. G. A. & Fagiolo, G. Propagation of economic shocks in input-output networks: A cross-country analysis (2014). [1401.4704](https://doi.org/10.1016/j.econbase.2014.04.004).
24. Acemoglu, D., Carvalho, V. M., Ozdaglar, A. & Tahbaz-Salehi, A. The network origins of aggregate fluctuations. *Econometrica* **80**, 1977–2016, DOI: <https://doi.org/10.3982/ECTA9623> (2012).
25. Carvalho, V. M. & Tahbaz-Salehi, A. Production networks: A primer. *Annu. Rev. Econ.* **11**, 635–663, DOI: <https://doi.org/10.1146/annurev-economics-080218-030212> (2019).
26. Gabaix, X. The granular origins of aggregate fluctuations. *Econometrica* **79**, 733–772, DOI: <https://doi.org/10.3982/ECTA8769> (2011).
27. Bacilieri, A., Borsos, A., Astudillo-Estevez, P. & Lafond, F. Firm-level production networks: what do we (really) know? Tech. Rep. 2023-08, INET Oxford Working Paper (2023).
28. Morimoto, Y. On aggregation problems in input-output analysis. *The Rev. Econ. Stud.* **37**, 119–126, DOI: [10.2307/2296502](https://doi.org/10.2307/2296502) (1970).
29. Diem, C., Borsos, A., Reisch, T., Kertész, J. & Thurner, S. Estimating the loss of economic predictability from aggregating firm-level production networks. *PNAS nexus* **3**, pgae064, DOI: <https://doi.org/10.1093/pnasnexus/pgae064> (2024).
30. Craighead, C. W., Blackhurst, J., Rungtusanatham, M. J. & Handfield, R. B. The Severity of Supply Chain Disruptions: Design Characteristics and Mitigation Capabilities. *Decis. Sci.* **38**, 131–156, DOI: <https://doi.org/10.1111/j.1540-5915.2007.00151.x> (2007).
31. Świerczek, A. The impact of supply chain integration on the “snowball effect” in the transmission of disruptions: An empirical evaluation of the model. *Int. J. Prod. Econ.* **157**, 89–104, DOI: <https://doi.org/10.1016/j.ijpe.2013.08.010> (2014). The International Society for Inventory Research, 2012.
32. Ivanov, D., Sokolov, B. & Dolgui, A. The ripple effect in supply chains: trade-off ‘efficiency-flexibility-resilience’ in disruption management. *Int. J. Prod. Res.* **52**, 2154–2172, DOI: <https://doi.org/10.1080/00207543.2013.858836> (2014).
33. Shao, B. B., Shi, Z. M., Choi, T. Y. & Chae, S. A data-analytics approach to identifying hidden critical suppliers in supply networks: Development of nexus supplier index. *Decis. Support. Syst.* **114**, 37–48, DOI: <https://doi.org/10.1016/j.dss.2018.08.008> (2018).
34. Käki, A., Salo, A. & Talluri, S. Disruptions in supply networks: A probabilistic risk assessment approach. *J. Bus. Logist.* **36**, 273–287, DOI: <https://doi.org/10.1111/jbl.12086> (2015).
35. Ledwoch, A., Brintrup, A., Mehnen, J. & Tiwari, A. Systemic risk assessment in complex supply networks. *IEEE Syst. J.* **12**, 1826–1837, DOI: [10.1109/JSYST.2016.2596999](https://doi.org/10.1109/JSYST.2016.2596999) (2018).
36. Diem, C., Borsos, A., Reisch, T., Kertész, J. & Thurner, S. Quantifying firm-level economic systemic risk from nation-wide supply networks. *Sci. reports* **12**, 1–13, DOI: <https://doi.org/10.1038/s41598-022-11522-z> (2022).
37. Wang, Y., Hong, A., Li, X. & Gao, J. Marketing innovations during a global crisis: A study of china firms’ response to covid-19. *J. Bus. Res.* **116**, 214–220, DOI: <https://doi.org/10.1016/j.jbusres.2020.05.029> (2020).

38. Belhadi, A. *et al.* Manufacturing and service supply chain resilience to the covid-19 outbreak: Lessons learned from the automobile and airline industries. *Technol. Forecast. Soc. Chang.* **163**, 120447, DOI: <https://doi.org/10.1016/j.techfore.2020.120447> (2021).
39. Klöckner, M., Schmidt, C. G., Wagner, S. M. & Swink, M. Firms' responses to the covid-19 pandemic. *J. Bus. Res.* **158**, 113664, DOI: <https://doi.org/10.1016/j.jbusres.2023.113664> (2023).
40. Zhao, K., Zuo, Z. & Blackhurst, J. V. Modelling supply chain adaptation for disruptions: An empirically grounded complex adaptive systems approach. *J. Oper. Manag.* **65**, 190–212, DOI: <https://doi.org/10.1002/joom.1009> (2019).
41. Bode, C., Wagner, S. M., Petersen, K. J. & Ellram, L. M. Understanding responses to supply chain disruptions: Insights from information processing and resource dependence perspectives. *Acad. Manag. J.* **54**, 833–856, DOI: [10.5465/amj.2011.64870145](https://doi.org/10.5465/amj.2011.64870145) (2011).
42. Bode, C. & Macdonald, J. R. Stages of supply chain disruption response: Direct, constraining, and mediating factors for impact mitigation. *Decis. Sci.* **48**, 836–874, DOI: <https://doi.org/10.1111/decis.12245> (2017).
43. Krammer, S. M. Navigating the new normal: Which firms have adapted better to the covid-19 disruption? *Technovation* **110**, 102368, DOI: <https://doi.org/10.1016/j.technovation.2021.102368> (2022).
44. Sabahi, S. & Parast, M. M. Firm innovation and supply chain resilience: a dynamic capability perspective. *Int. J. Logist. Res. Appl.* **23**, 254–269, DOI: [10.1080/13675567.2019.1683522](https://doi.org/10.1080/13675567.2019.1683522) (2020).
45. Xu, Z., Elomri, A., Kerbache, L. & El Omri, A. Impacts of covid-19 on global supply chains: Facts and perspectives. *IEEE Eng. Manag. Rev.* **48**, 153–166, DOI: [10.1109/EMR.2020.3018420](https://doi.org/10.1109/EMR.2020.3018420) (2020).
46. Panwar, R., Pinkse, J. & Marchi, V. D. The future of global supply chains in a post-covid-19 world. *California Manag. Rev.* **64**, 5–23, DOI: [10.1177/00081256211073355](https://doi.org/10.1177/00081256211073355) (2022).
47. Squartini, T. & Garlaschelli, D. Analytical maximum-likelihood method to detect patterns in real networks. *New J. Phys.* **13**, 083001, DOI: <https://doi.org/10.1088/1367-2630/13/8/083001> (2011).
48. Cimini, G. *et al.* The statistical physics of real-world networks. *Nat. Rev. Phys.* **1**, 58–71, DOI: <https://doi.org/10.1038/s42254-018-0002-6> (2019).
49. Squartini, T., Van Lelyveld, I. & Garlaschelli, D. Early-warning signals of topological collapse in interbank networks. *Sci. Reports* **3**, 3357, DOI: <https://doi.org/10.1038/srep03357> (2013).
50. Gualdi, S., Cimini, G., Primicerio, K., Di Clemente, R. & Challet, D. Statistically validated network of portfolio overlaps and systemic risk. *Sci. Reports* **6**, 39467, DOI: [10.1038/srep39467](https://doi.org/10.1038/srep39467) (2016).
51. Cimini, G., Carra, A., Didomenicantonio, L. & Zaccaria, A. Meta-validation of bipartite network projections. *Commun. Phys.* **5**, 76, DOI: [10.1038/s42005-022-00856-9](https://doi.org/10.1038/s42005-022-00856-9) (2022).
52. Pratelli, M., Saracco, F. & Petrocchi, M. Entropy-based detection of twitter echo chambers. *PNAS Nexus* **3**, pgae177, DOI: [10.1093/pnasnexus/pgae177](https://doi.org/10.1093/pnasnexus/pgae177) (2024). <https://academic.oup.com/pnasnexus/article-pdf/3/5/pgae177/58004712/pgae177.pdf>.
53. Ferracci, A. & Cimini, G. Systemic risk in interbank networks: disentangling balance sheets and network effects (2022). [2109.14360](https://doi.org/10.2109.14360).
54. Ialongo, L. N. *et al.* Reconstructing firm-level interactions in the dutch input–output network from production constraints. *Sci. Reports* **12**, 1–12, DOI: <https://doi.org/10.1038/s41598-022-13996-3> (2022).
55. Fessina, M. *et al.* Inferring firm-level supply chain networks with realistic systemic risk from industry sector-level data (2024). [2408.02467](https://doi.org/10.2408.02467).
56. Bargigli, L., Lionetto, A. & Viaggiu, S. A statistical test of walrasian equilibrium by means of complex networks theory. *J. Stat. Phys.* **165**, 351–370 (2016).
57. Bardoscia, M. *et al.* The physics of financial networks. *Nat. Rev. Phys.* **3**, 490–507, DOI: [10.1038/s42254-021-00322-5](https://doi.org/10.1038/s42254-021-00322-5) (2021).
58. Borsos, A. & Stancsics, M. Unfolding the hidden structure of the Hungarian multi-layer firm network. Tech. Rep., Magyar Nemzeti Bank (Central Bank of Hungary) (2020).
59. EUROSTAT. Your companion guide to international statistical classifications. section iv - description of the main economic classifications (2021).
60. Serafino, M. *et al.* True scale-free networks hidden by finite size effects. *Proc. Natl. Acad. Sci.* **118**, e2013825118, DOI: [10.1073/pnas.2013825118](https://doi.org/10.1073/pnas.2013825118) (2021). <https://www.pnas.org/doi/pdf/10.1073/pnas.2013825118>.

61. Reisch, T., Borsos, A. & Thurner, S. Supply chain network rewiring dynamics at the firm-level, DOI: [10.48550/arXiv.2503.20594](https://doi.org/10.48550/arXiv.2503.20594) (2025).
62. Gabrielli, A., Macchiati, V. & Garlaschelli, D. Critical density for network reconstruction. In *From Computational Logic to Computational Biology: Essays Dedicated to Alfredo Ferro to Celebrate His Scientific Career*, 223–249, DOI: https://doi.org/10.1007/978-3-031-55248-9_11 (Springer, 2024).
63. Gottschalk, F. & Lehmann, A. *Covid-19 and Swiss Post: Volume Developments and the Economic Value of Postal Service, in the Pandemic and Beyond*, 207–222 (Springer International Publishing, Cham, 2023).
64. Halpern, L., Koren, M. & Szeidl, A. Imported inputs and productivity. *Am. economic review* **105**, 3660–3703 (2015).
65. Juhász, S., Elekes, Z., Ilyés, V. & Neffke, F. Colocation of skill related suppliers—revisiting coagglomeration using firm-to-firm network data. *arXiv preprint arXiv:2405.07071* (2024).
66. Zelbi, G., Ialongo, L. N. & Thurner, S. Systemic risk mitigation in supply chains through network rewiring (2025). [2504.12955](https://doi.org/10.12575.2504.12955).
67. Pichler, A., Pangallo, M., del Rio-Chanona, R. M., Lafond, F. & Farmer, J. D. In and out of lockdown: Propagation of supply and demand shocks in a dynamic input-output model. *arXiv preprint arXiv:2102.09608* DOI: <https://doi.org/10.48550/arXiv.2102.09608> (2021).
68. Mastrandrea, R., Squartini, T., Fagiolo, G. & Garlaschelli, D. Enhanced reconstruction of weighted networks from strengths and degrees. *New J. Phys.* **16**, 043022, DOI: <https://doi.org/10.1088/1367-2630/16/4/043022> (2014).
69. Gabrielli, A., Mastrandrea, R., Caldarelli, G. & Cimini, G. Grand canonical ensemble of weighted networks. *Phys. Rev. E* **99**, 030301, DOI: <https://doi.org/10.1103/PhysRevE.99.030301> (2019).
70. Cimini, G., Squartini, T., Garlaschelli, D. & Gabrielli, A. Systemic risk analysis on reconstructed economic and financial networks. *Sci. Reports* **5**, DOI: <https://doi.org/10.1038/srep15758> (2015).
71. Parisi, F., Squartini, T. & Garlaschelli, D. A faster horse on a safer trail: generalized inference for the efficient reconstruction of weighted networks. *New J. Phys.* **22**, 053053, DOI: <https://doi.org/10.1088/1367-2630/ab74a7> (2020).
72. Park, J. & Newman, M. E. Statistical mechanics of networks. *Phys. Rev. E* **70**, 066117, DOI: <https://doi.org/10.1103/PhysRevE.70.066117> (2004).
73. Caldarelli, G., Capocci, A., De Los Rios, P. & Munoz, M. A. Scale-free networks from varying vertex intrinsic fitness. *Phys. Rev. Lett.* **89**, 258702, DOI: <https://doi.org/10.1103/PhysRevLett.89.258702> (2002).
74. Garlaschelli, D. & Loffredo, M. I. Fitness-dependent topological properties of the world trade web. *Phys. Rev. Lett.* **93**, 188701, DOI: <https://doi.org/10.1103/PhysRevLett.93.188701> (2004).

Acknowledgements

A.M. and G.C. acknowledge financial support from the National Recovery and Resilience Plan (NRRP), Mission 4 Component 2 Investment 1.1, funded by the European Union - NextGenerationEU: Call for tender No. 104 of 02/02/2022 by the Italian Ministry of University and Research (MUR), Project Title: *RENet - Reconstructing economic networks: from physics to machine learning and back*, Concession Decree No. 957 of 30/06/2023, Project code 2022MTBB22 - CUP E53D23001770006; Call for tender No. 1409 of 14/09/2022 by the Italian Ministry of University and Research (MUR), Project Title: *C2T - From Crises to Theory: towards a science of resilience and recovery for economic and financial systems*, Concession Decree No. 1381 of 01/09/2023, Project code P2022E93B8 - CUP E53D23018320001.

B.L. acknowledges financial support from the Hungarian National Scientific Fund (OTKA K 138970).

R.D.C. acknowledges support from the Lagrange Project of the ISI Foundation funded by CRT Foundation.

This manuscript was prepared using the datasets of the Central Statistical Office on firm-to-firm VAT transactions and firm import-export. The calculations contained in the document and the conclusions drawn from them are exclusively the intellectual products of Anna Mancini, Balázs Lengyel, Riccardo Di Clemente and Giulio Cimini as the authors.

Author contributions statement

Study conception and design: BL, RDC, GC. Data analysis: AM, BL. Contributed methods: AM, GC. Discussion and interpretation of results: AM, BL, RDC, GC. Manuscript preparation: AM, BL, RDC, GC.

Competing interests

The authors declare no competing interests.

Evolution and determinants of firm-level systemic risk in local production networks

Anna Mancini, Balázs Lengyel, Riccardo Di Clemente, Giulio Cimini

Supplementary Materials

S1 Filtering procedure

Figure S5A shows that the majority of firms' headquarters are based in Budapest. Figure S5B instead shows the number of employees versus the firm's ESRI value before applying the last filter on the number of employees and the degree. The two variables are very correlated, thus firms with fewer employees also show lower ESRI scores. All firms that satisfy the condition on employees (≤ 11) have a low value of systemic risk.

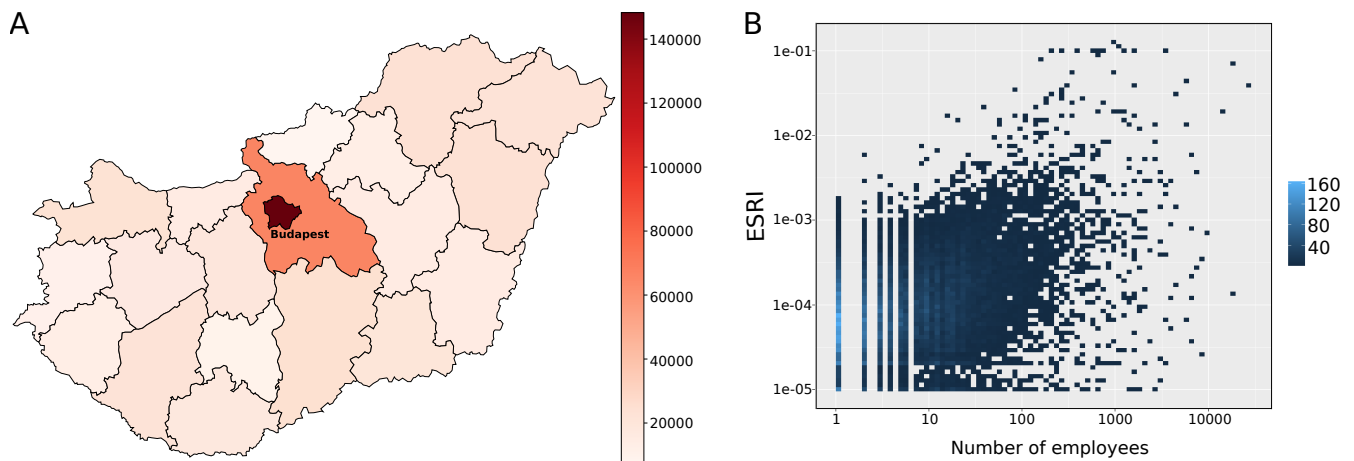


Figure S5. Filtering procedures. A) Hungarian NUTS3 counties colored by the number of firms that are based in each one, as of 2019. B) ESRI of each firm versus number of employees.

S2 NUTS3 aggregation of firms' sales

To proxy the GPD of the different Hungarian regions, we aggregate all transactions between firms on a NUTS3 level, resulting in a network where nodes are NUTS3 regions and links are all monetary transactions between them. Figure S6 shows the out-strength (total sales) for each region, where we can see how the Budapest area is responsible for around 48% of the total out-strength of all regions.

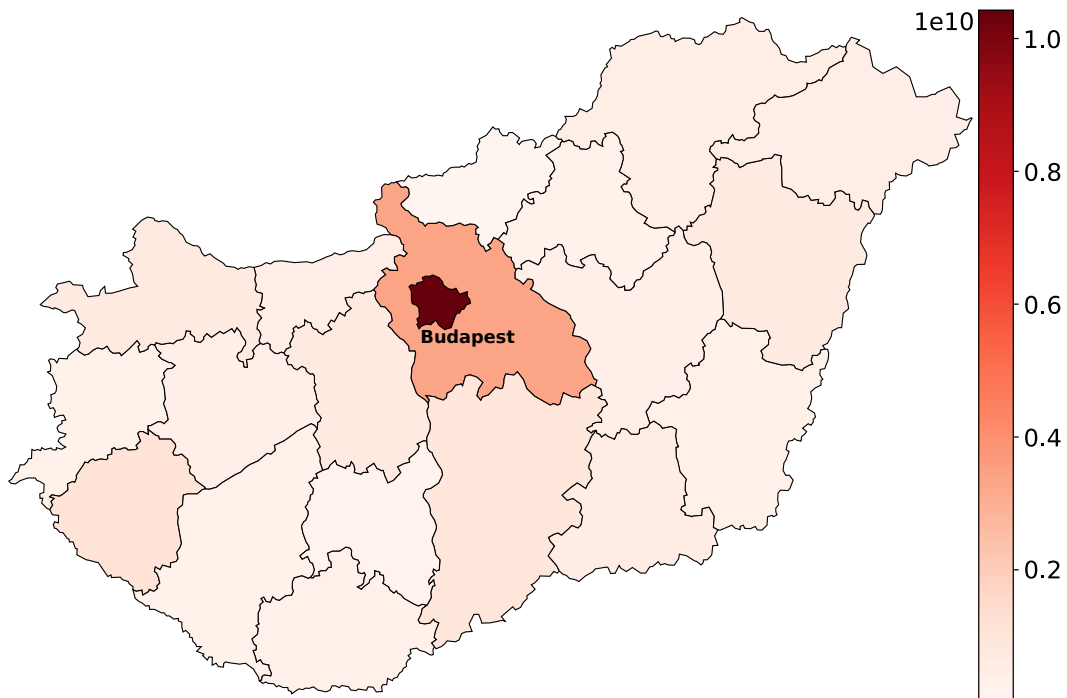


Figure S6. NUTS3 out-strength. Out-strength aggregated on a NUTS3 level, for all Hungarian regions.

S3 ESRI vs degree values

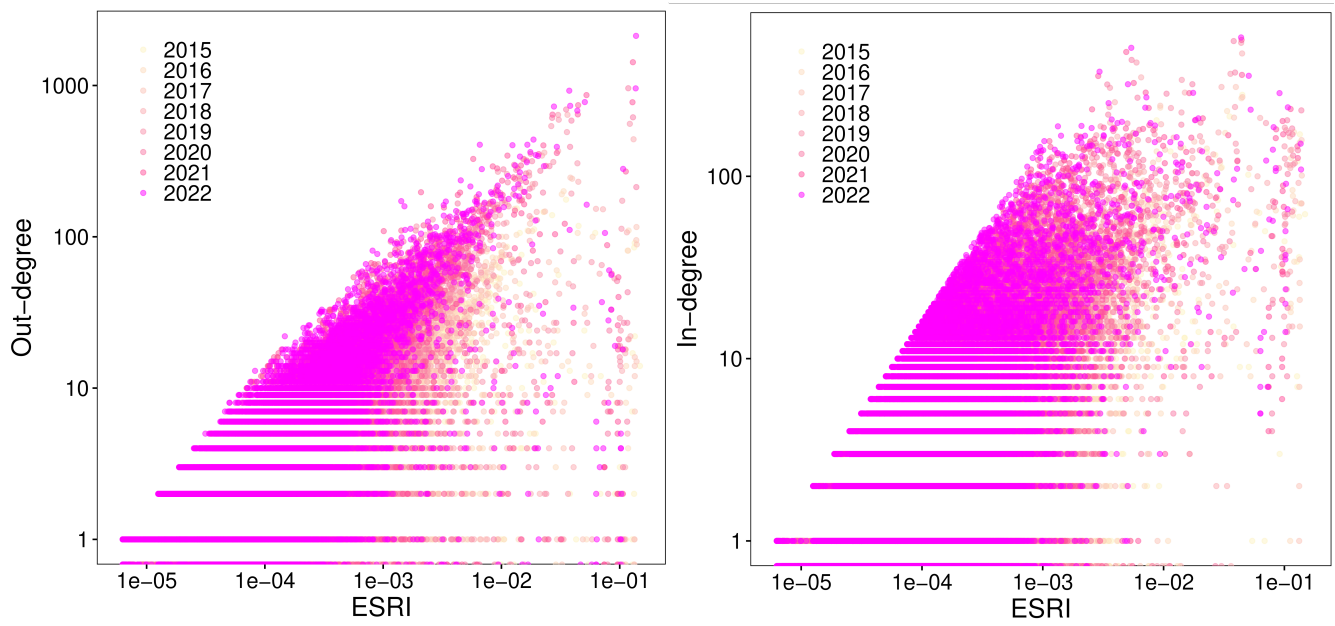


Figure S7. Scatter plot of ESRI values vs firm's in- and out-degree.

S4 ESRI vs strengths

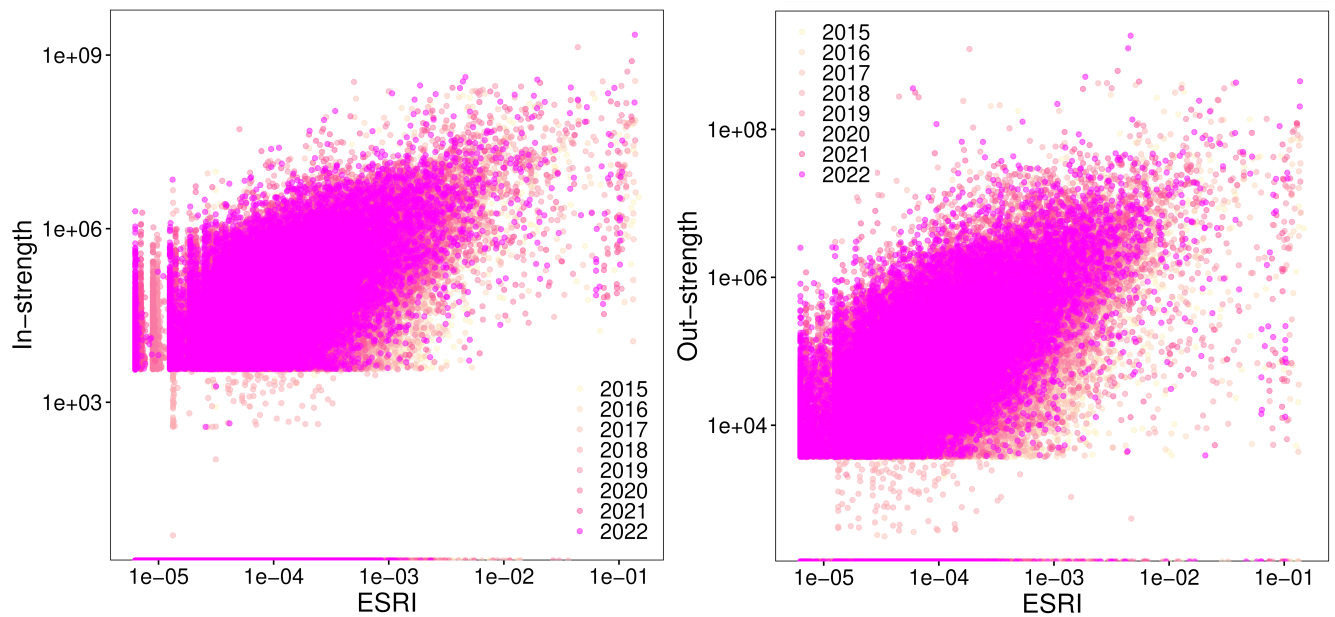


Figure S8. Scatter plot of ESRI values vs firm's in- and out-strengths.

S5 Correlation matrices of ESRI values

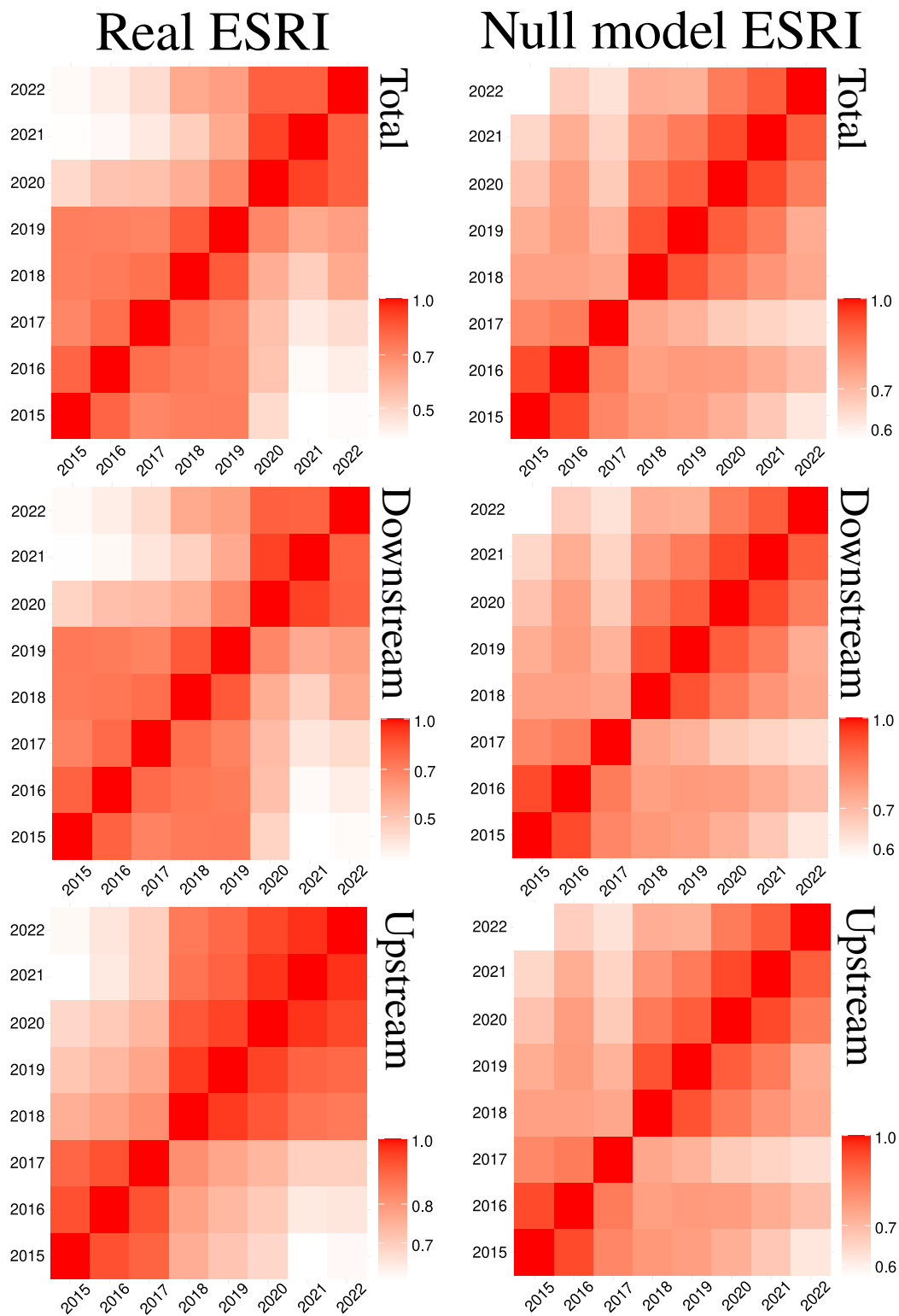


Figure S9. Correlation matrices of ESRI values for all years considered. Left column for empirical networks and right column for null models. First row shows matrices for the total ESRI values, second row for the downstream values and third row for the upstream values. It is worth noting how the upstream ESRI values show a disruption in 2018, hinting to a possible change in the structure of the network affecting mostly the in-strengths.

S6 ESRI empirical rankings for 2015-2022

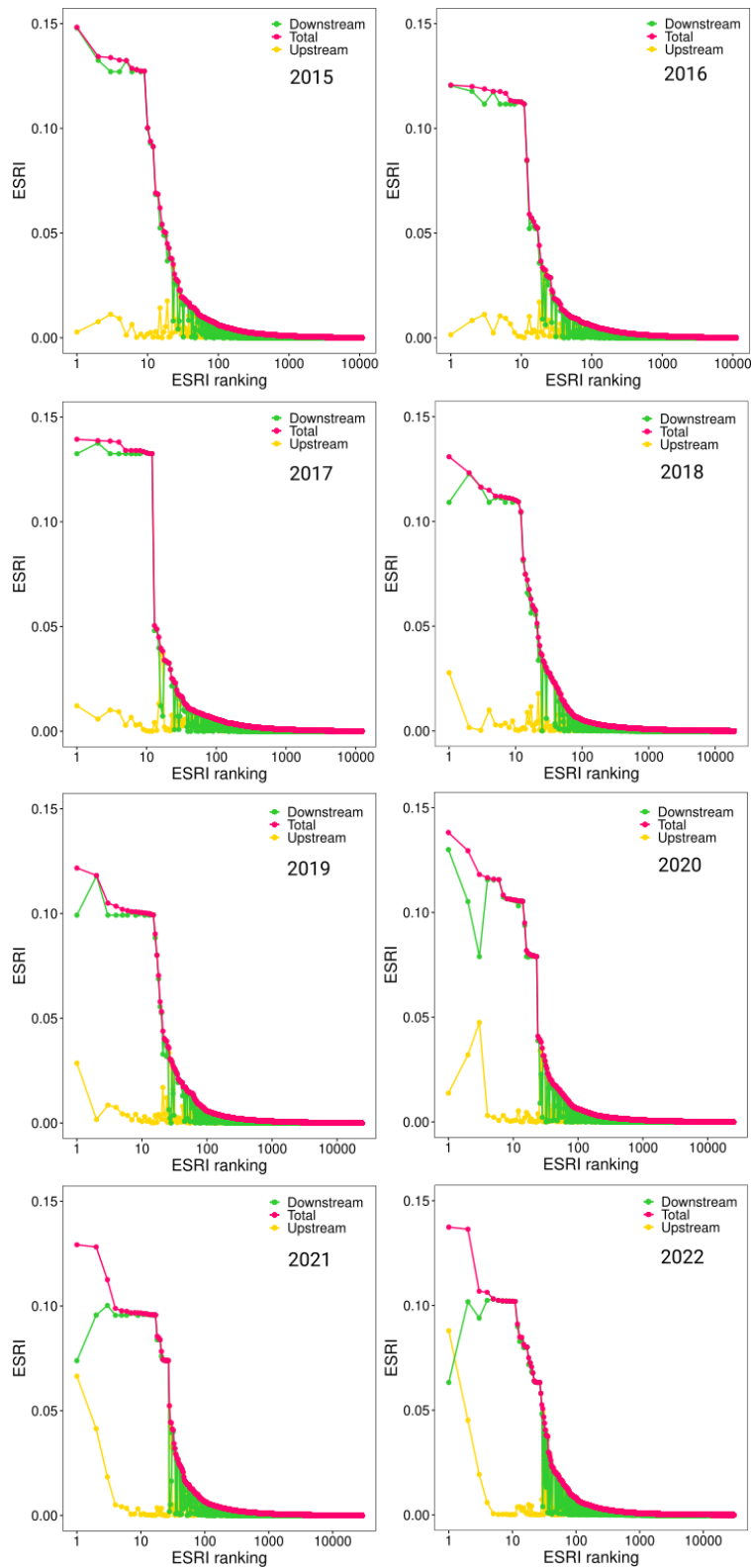
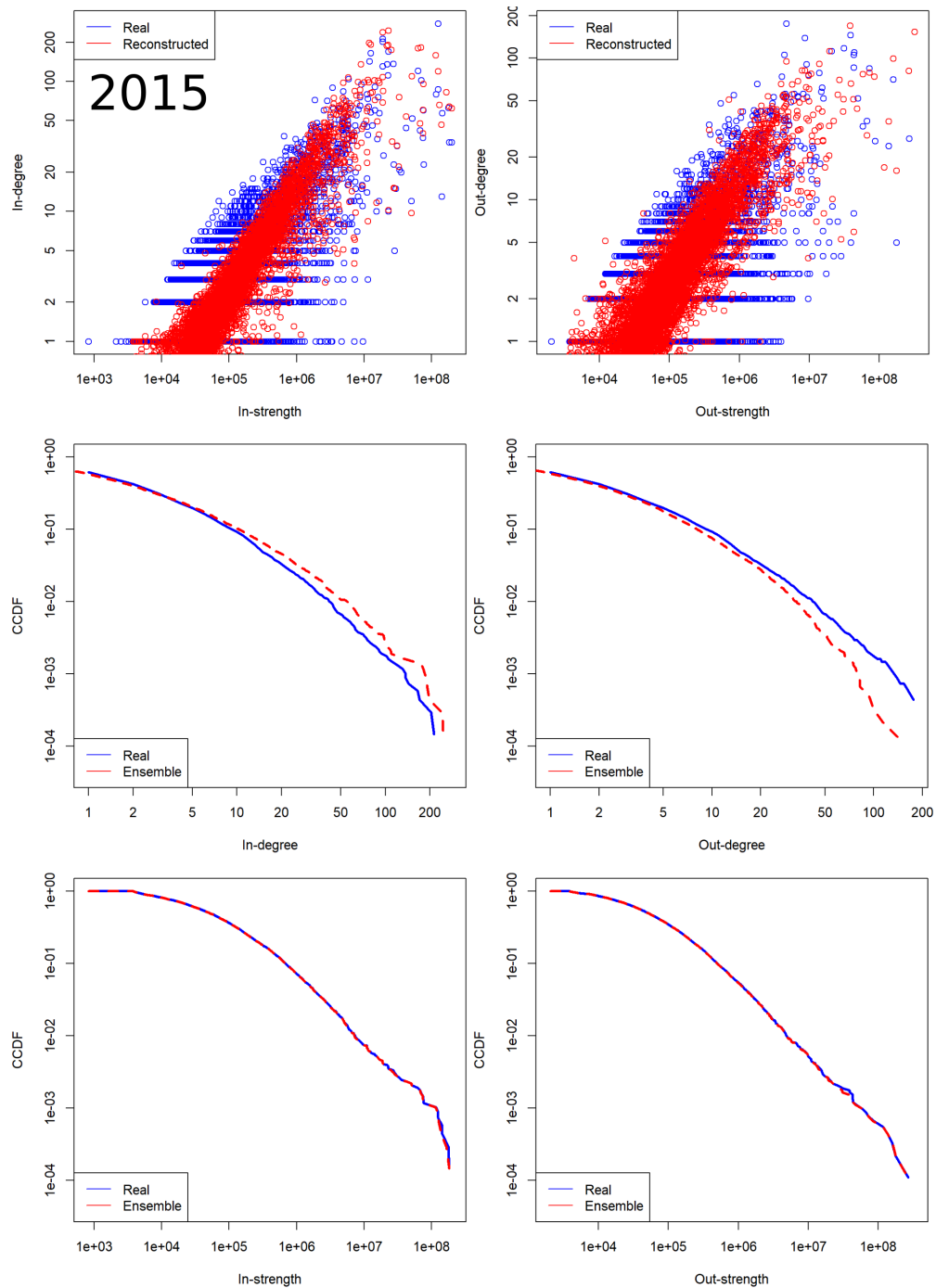
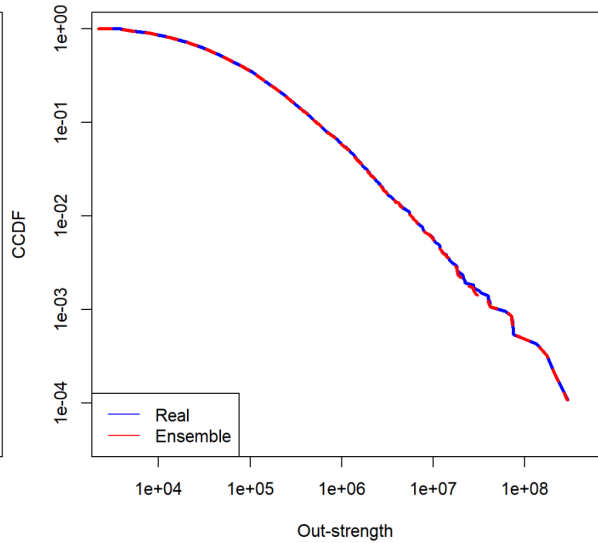
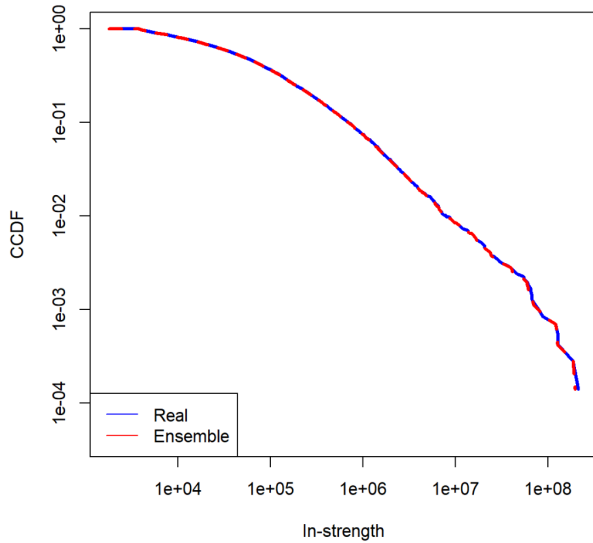
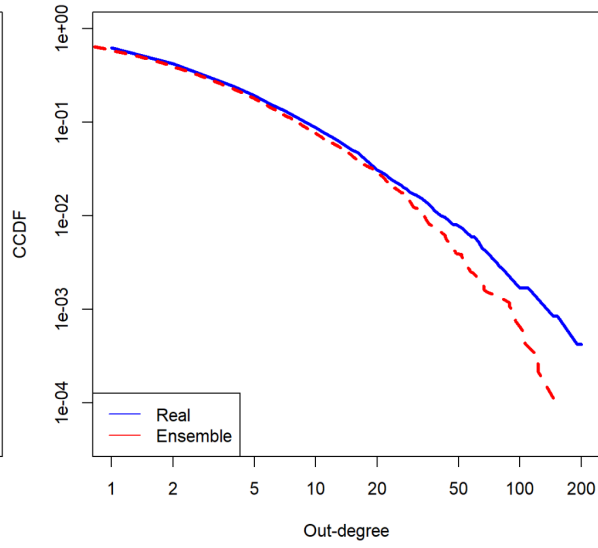
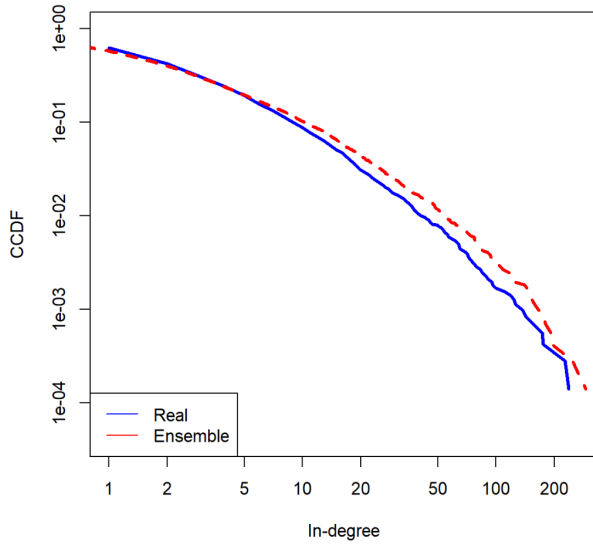
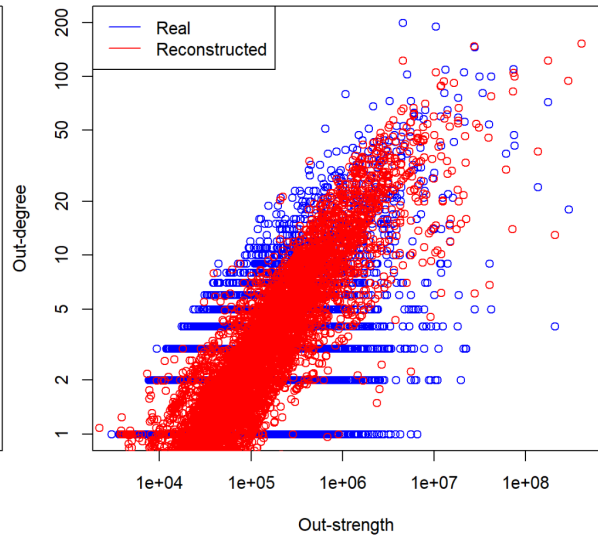
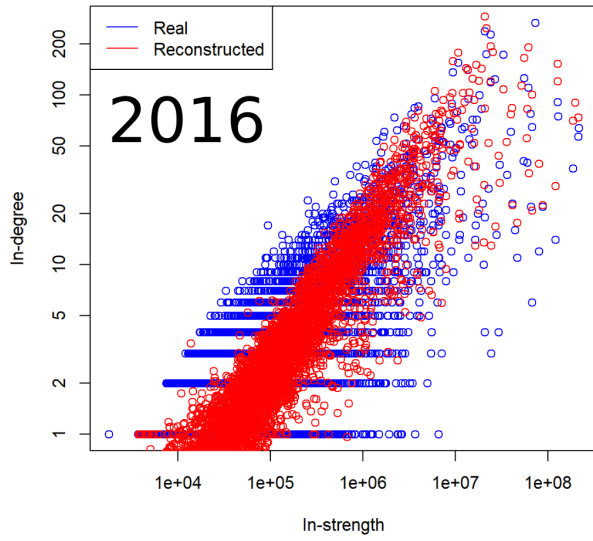


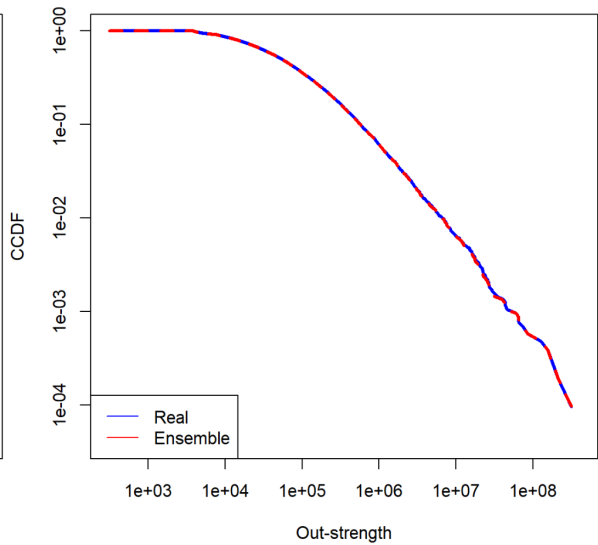
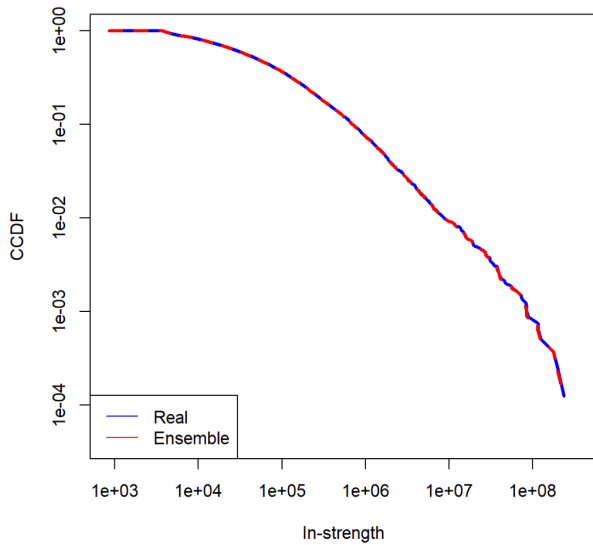
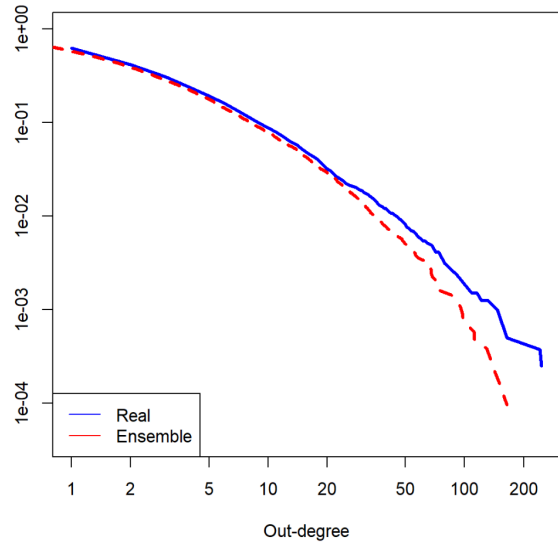
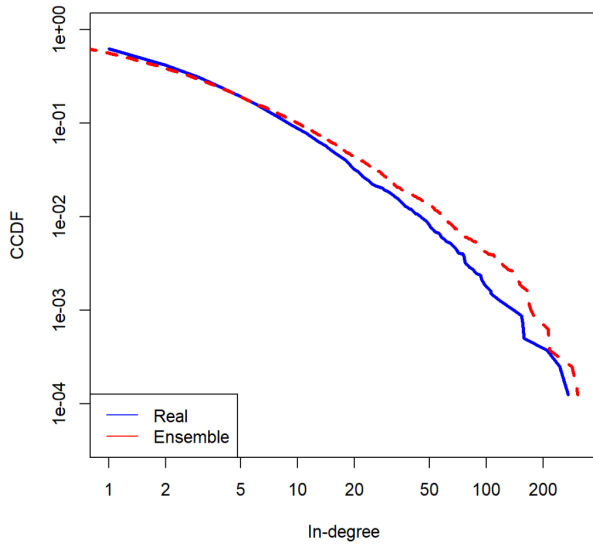
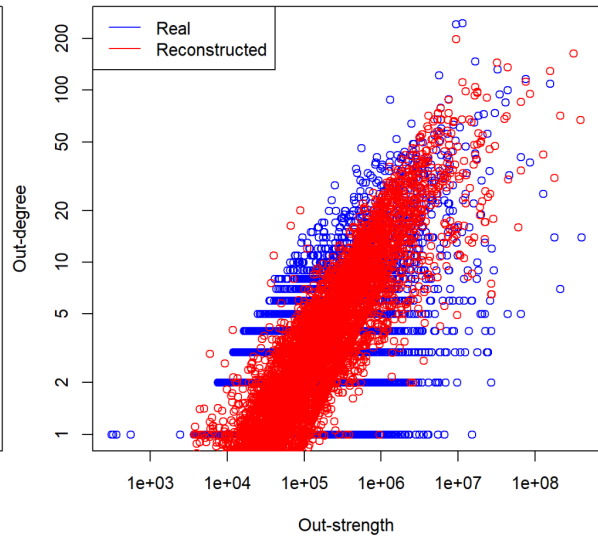
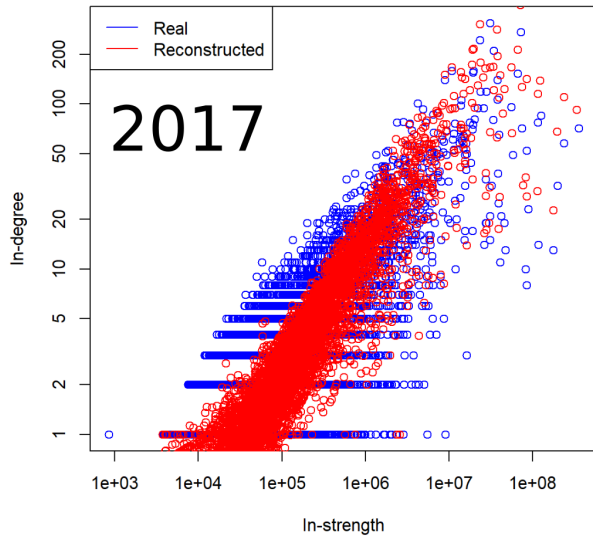
Figure S10. ESRI ranking for all empirical networks, from 2015 to 2022. In pink the total ESRI, in green the downstream values and in yellow the upstream values.

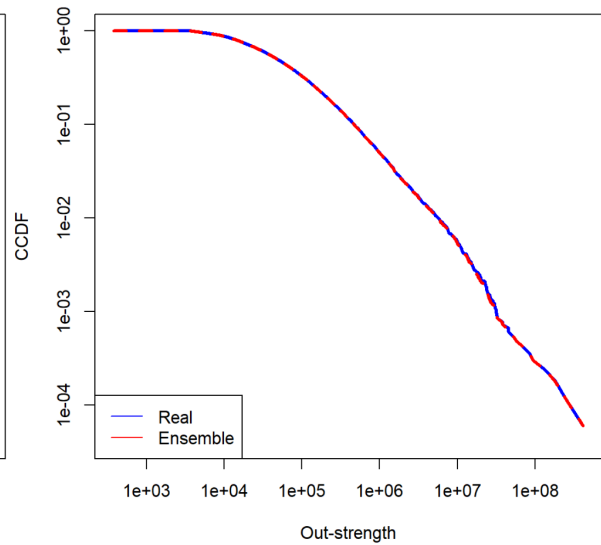
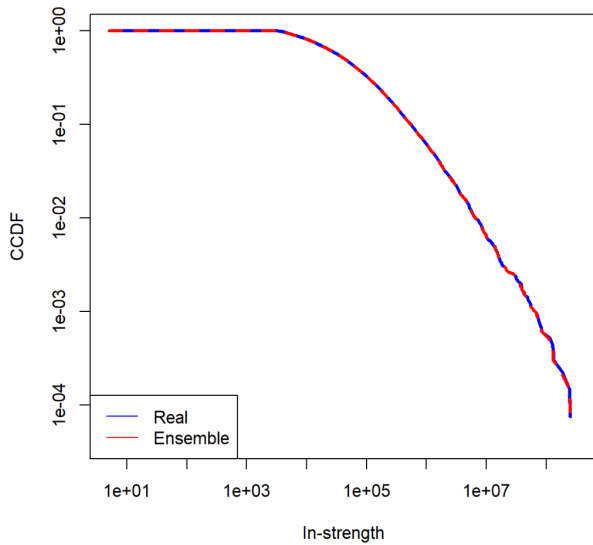
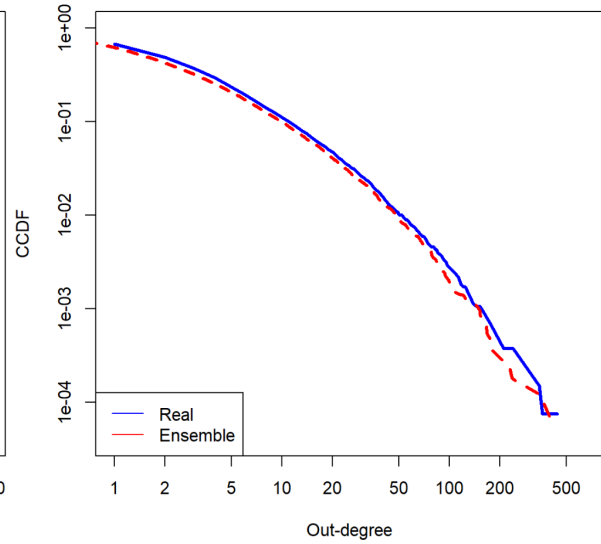
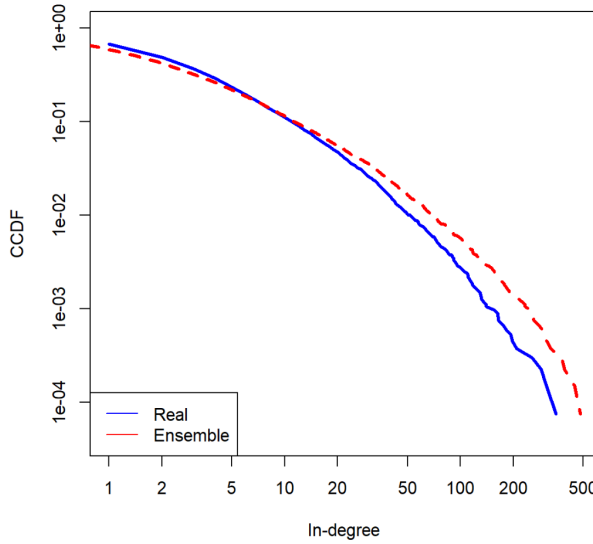
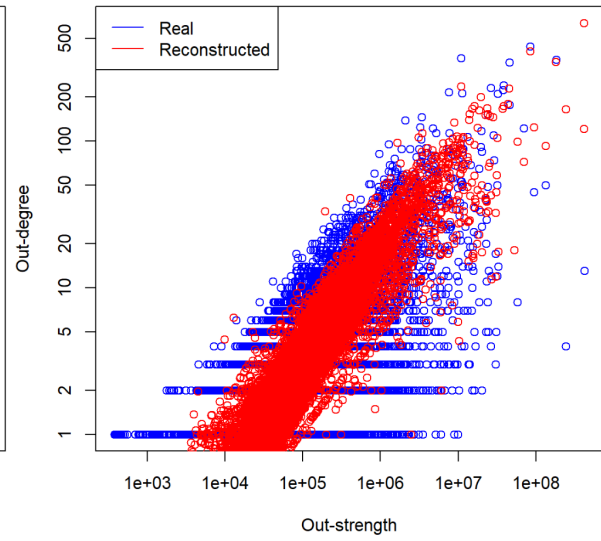
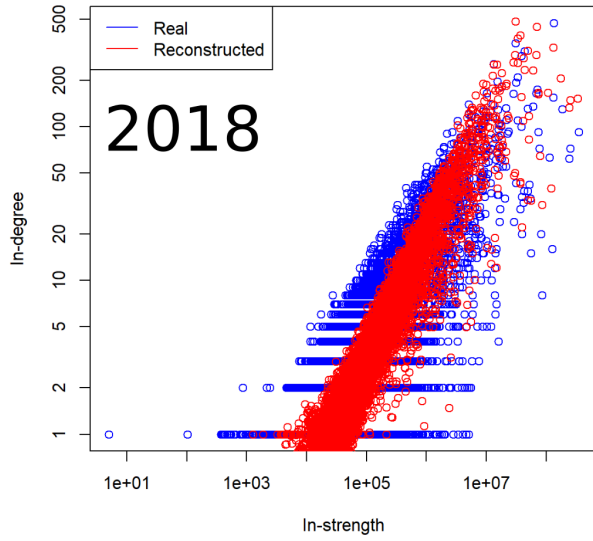
S7 Degree and strength statistics for empirical and null model networks

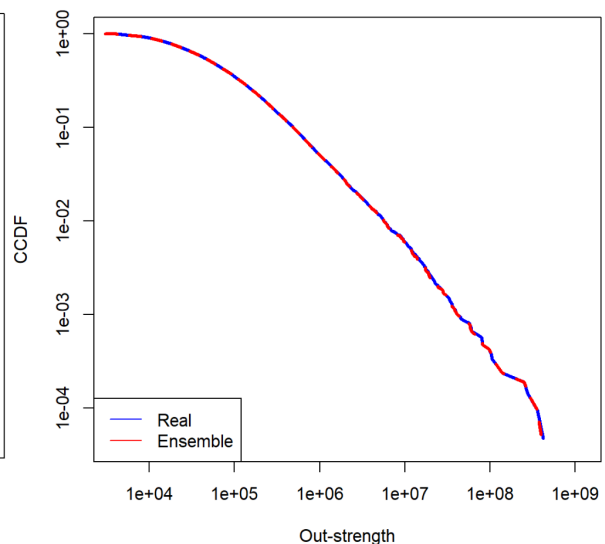
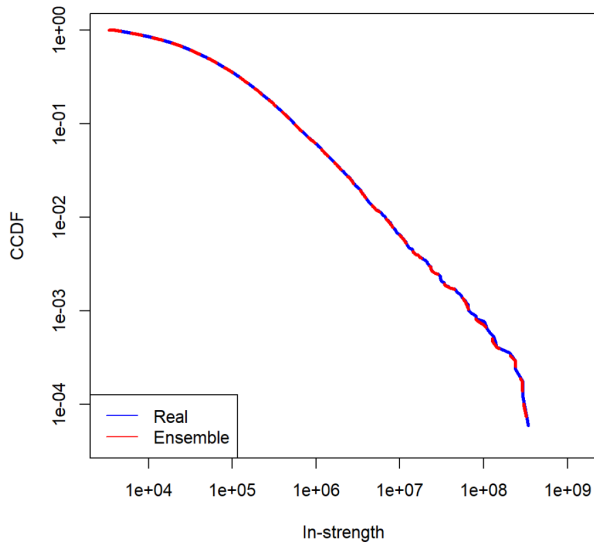
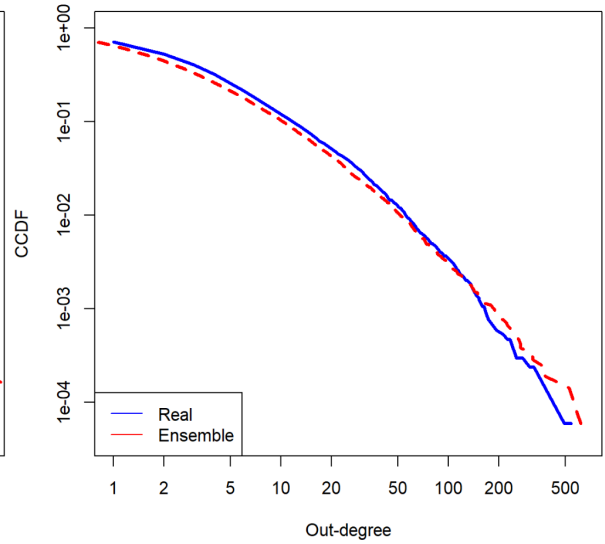
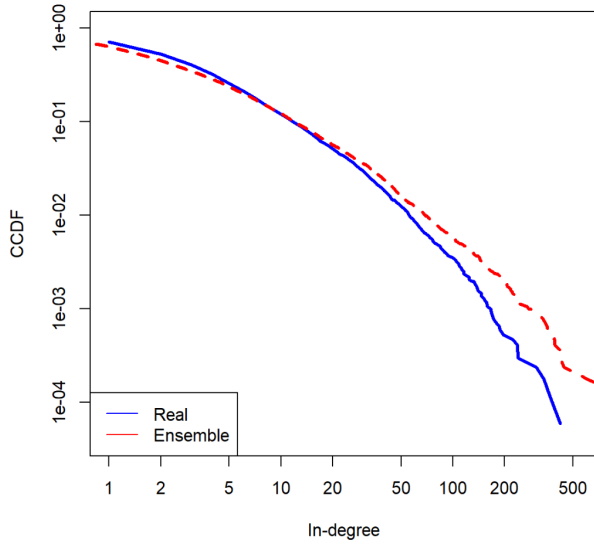
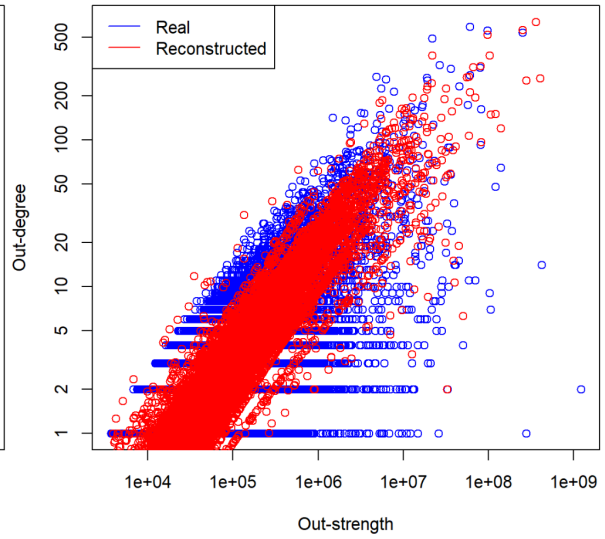
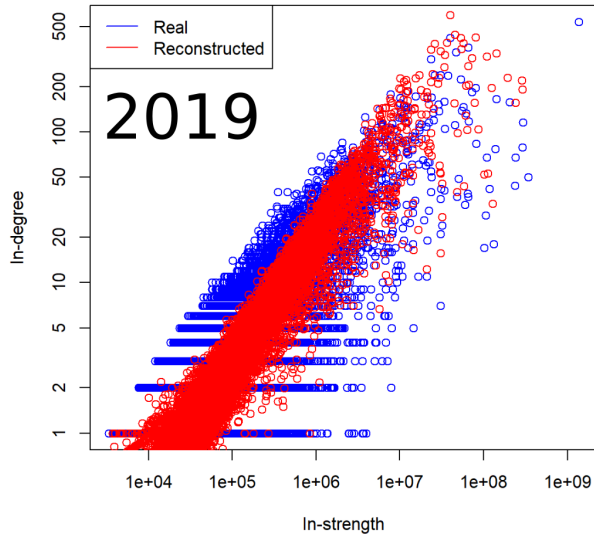
For each year, below we show the following plots. The first row is the scatter plot for the empirical (blue) in-/out-degree vs in-/out-strength and the null model (in red) in-/out-degree vs in-/out-strength, obtained as averages over the s-GM ensemble. The plots also verify the fitness ansatz, according to which the strengths are proportional to the degrees and can be used to infer them. Panels in the second row represent the complementary cumulative distributions for the in- and out-degrees for both real (blue solid line) and null model (red dashed line) networks. The overlap between the curves highlights the optimal result of the null models in reproducing the empirical degrees. Third row panels instead represent the complementary cumulative distributions for the in- and out-strengths for both real (blue solid line) and null model (red dashed line) networks. The two curves overlap completely, as strength values are constrained by the s-GM.

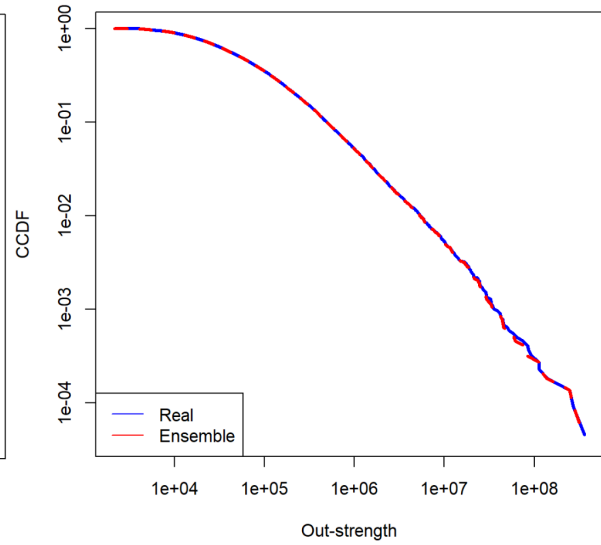
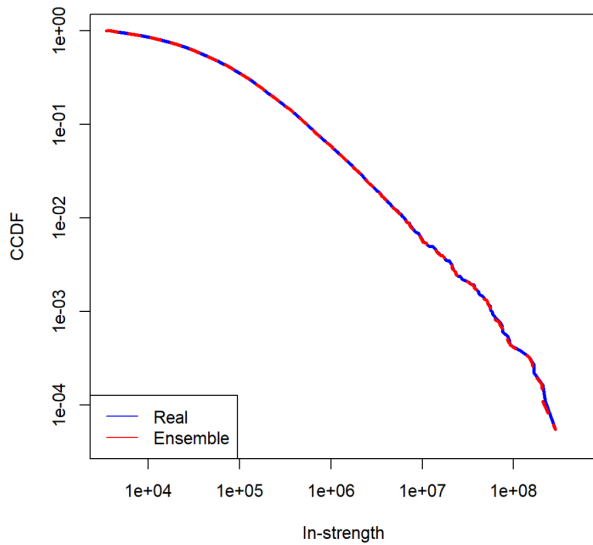
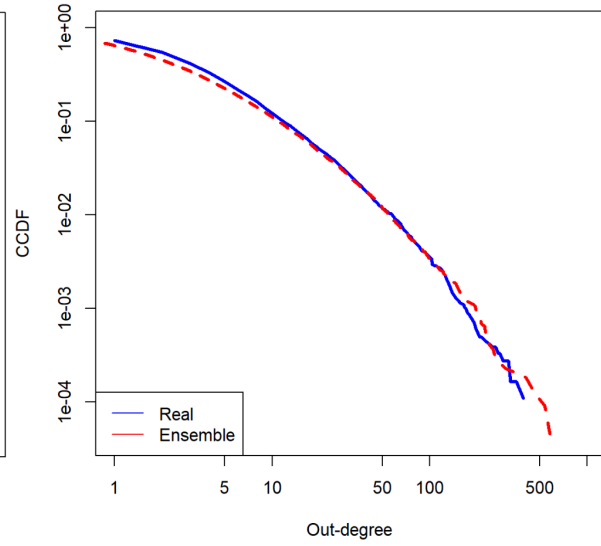
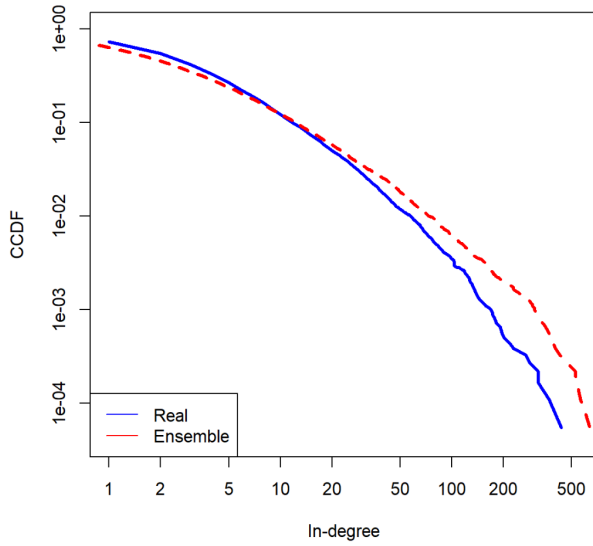
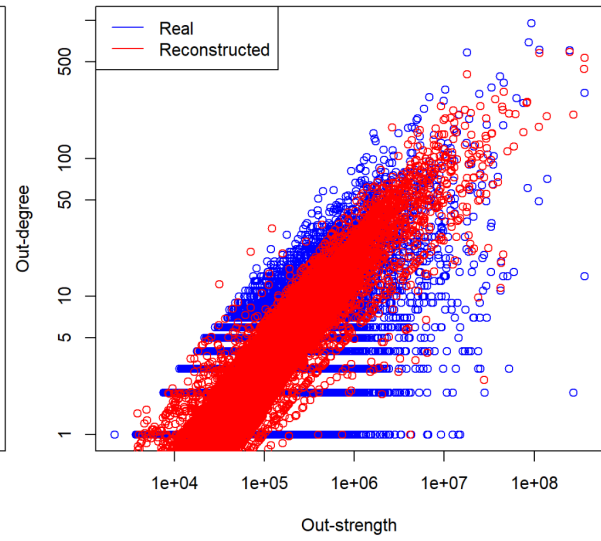
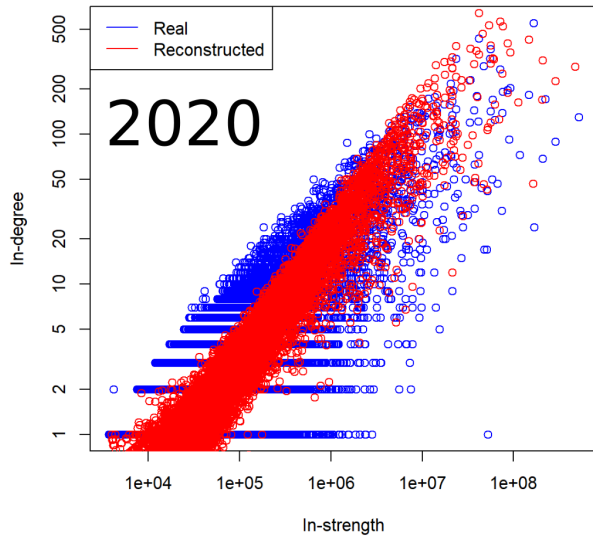


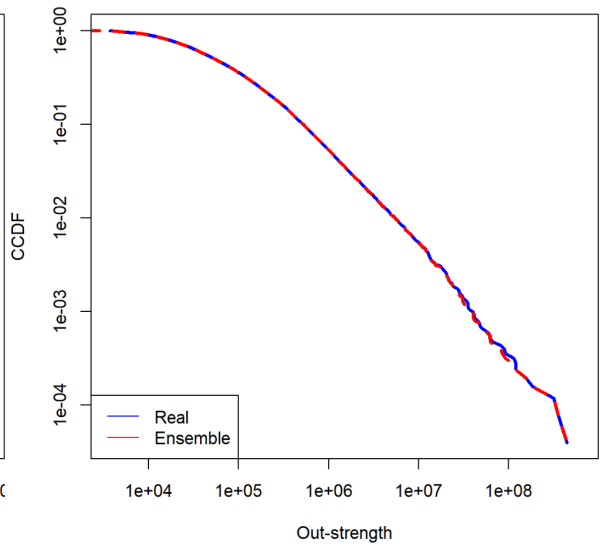
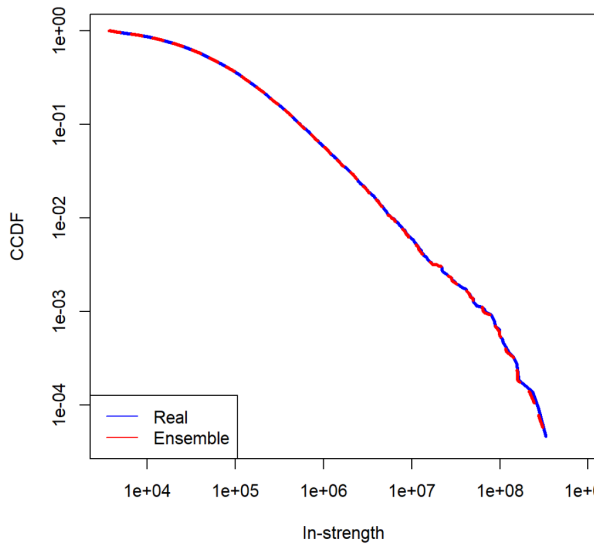
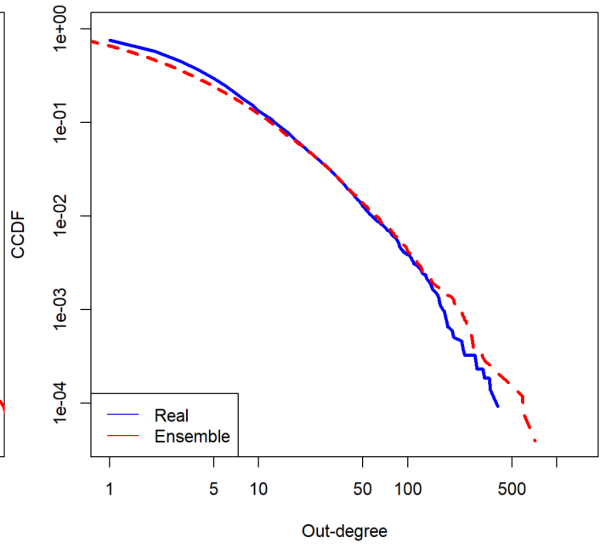
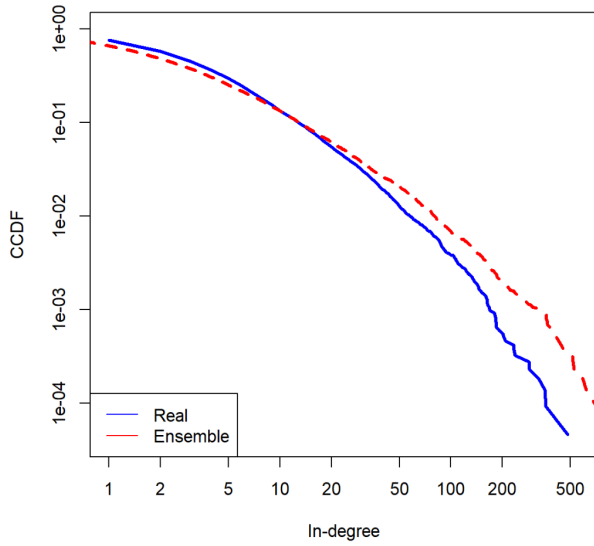
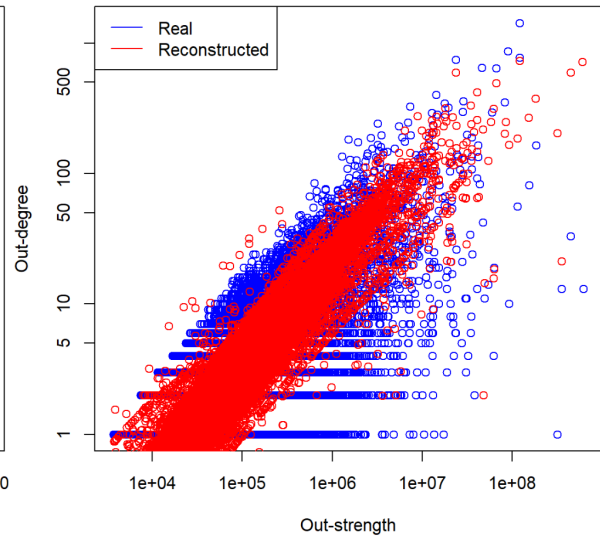
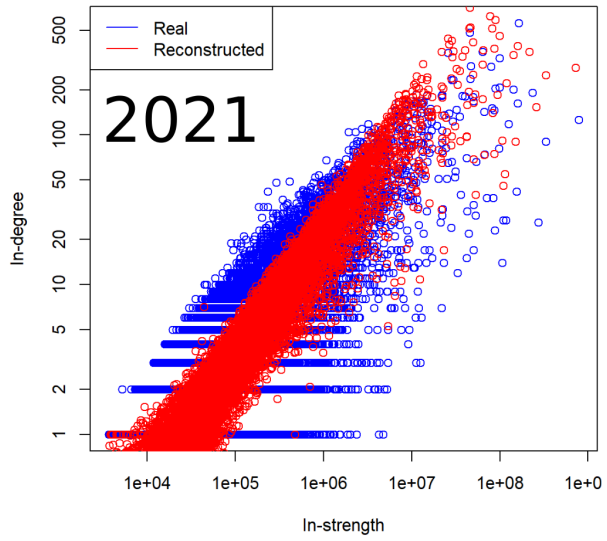


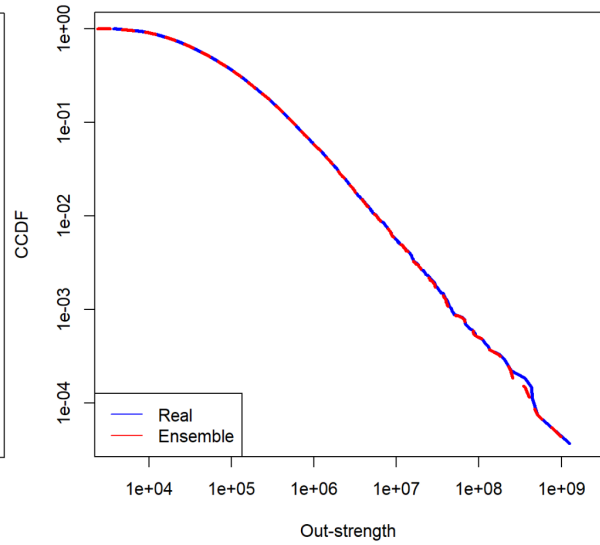
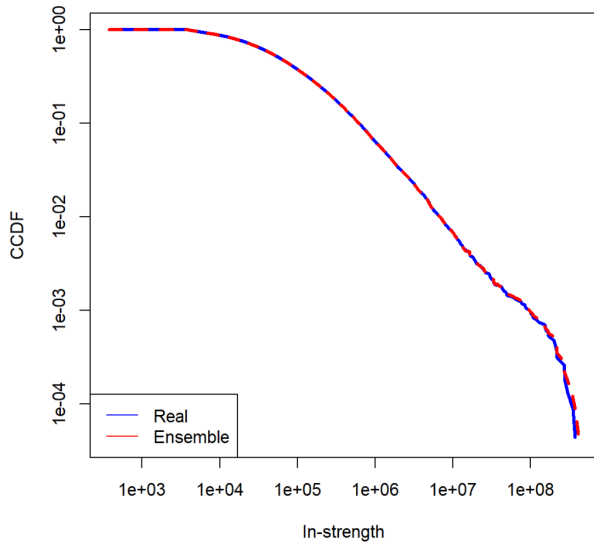
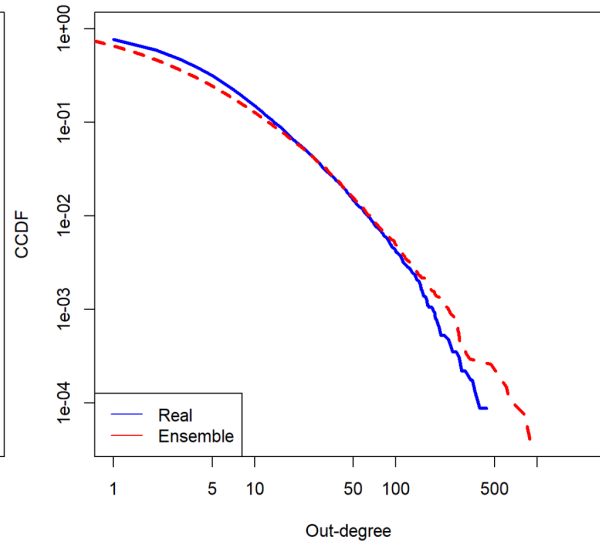
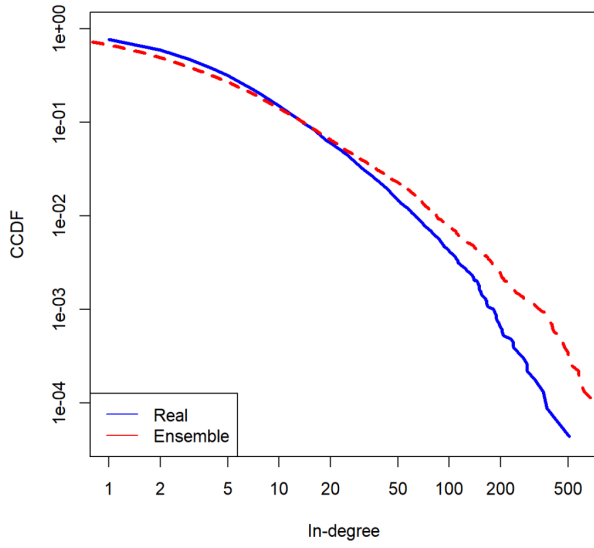
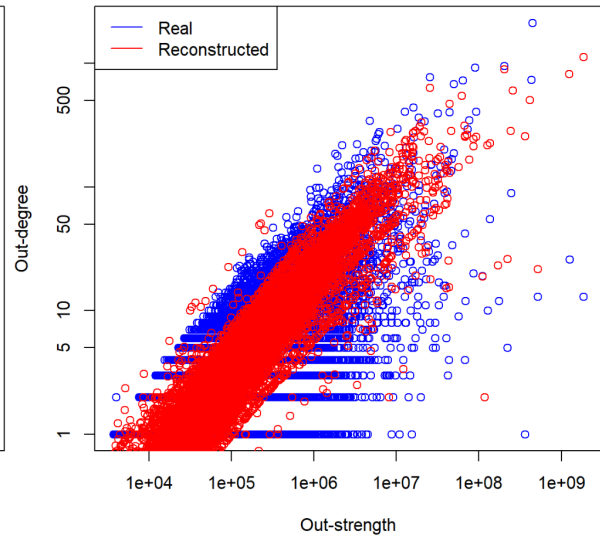
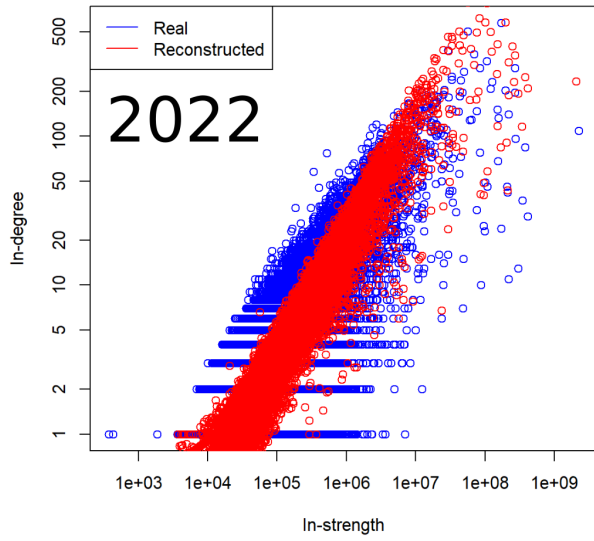












S8 Empirical vs null model values of ESRI for 2015-2022

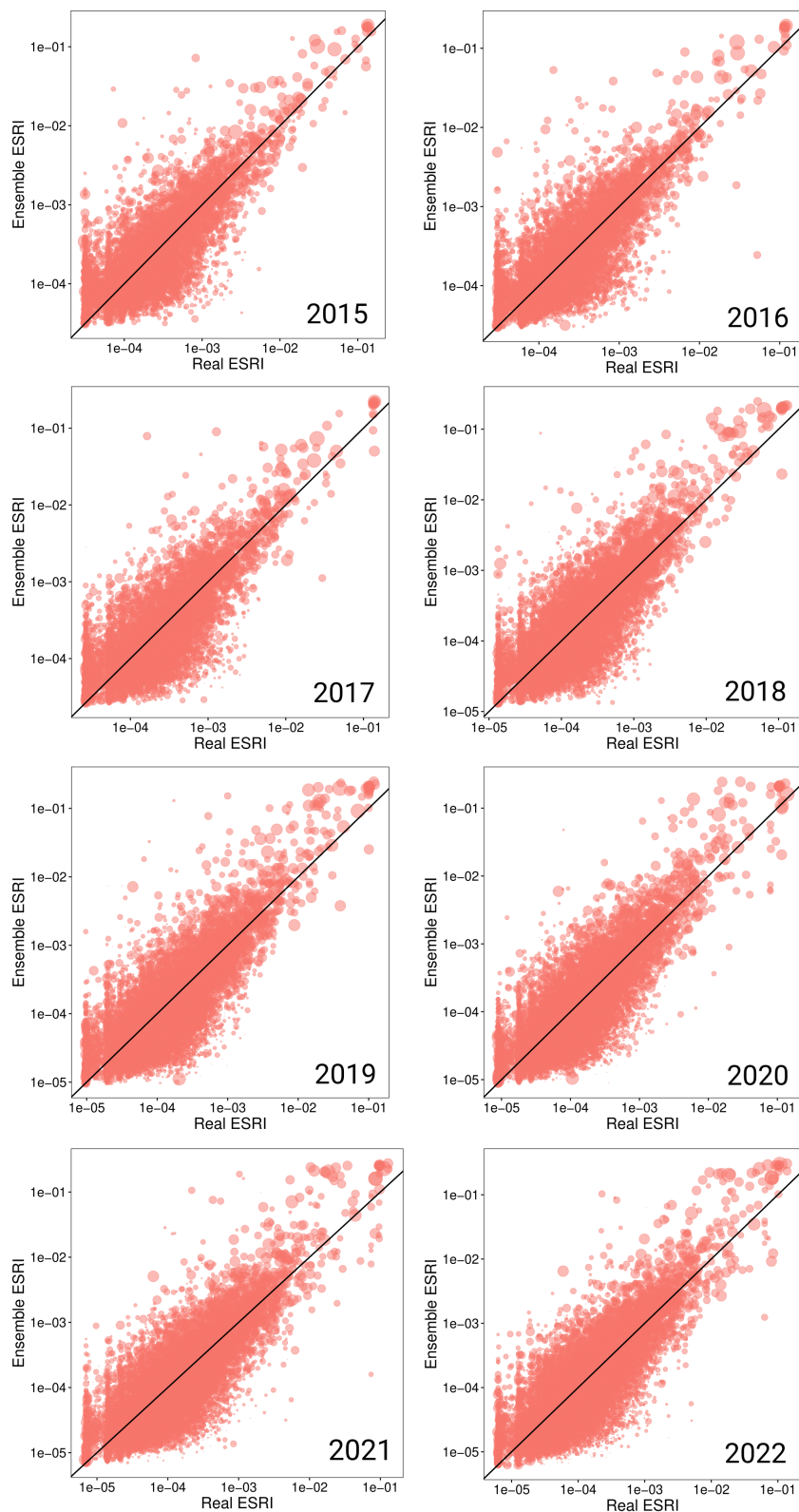


Figure S8. Scatter plots of empirical vs null model values of firm-level ESRI for all years, from 2015 to 2022. Dot size is proportional to the firm's number of employees.

S9 Empirical vs null model rankings of ESRI for 2015-2022

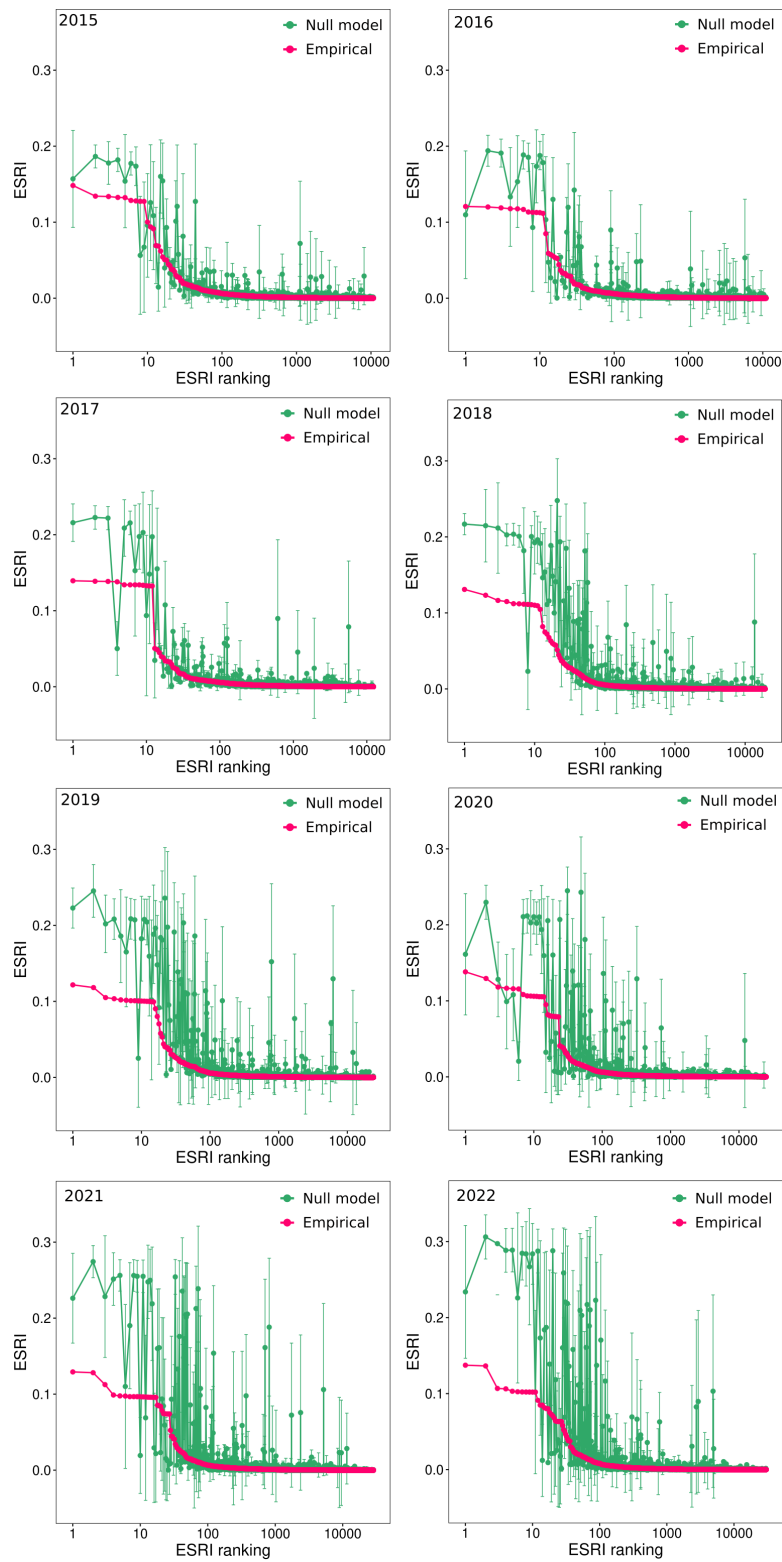


Figure S9. Ranking plots of empirical (pink) vs null model (green) values of ESRI for all years, from 2015 to 2022. As the years progress the two rankings become progressively divergent, underlying that the null model becomes less able to reproduce the empirical dynamics of firms.

S10 Difference of ESRI rankings for empirical and null model networks

To quantify the mismatch between real and null model ESRI values shown in the rankings of the previous section, we compute for each firm the absolute value of the difference between empirical $ESRI$ and null model $\langle ESRI \rangle$ scores, and rank them for each year in decreasing order. The higher the curve, the greater the mismatch between the values. As can be seen by the plot below, the highest differences occur during the COVID years.

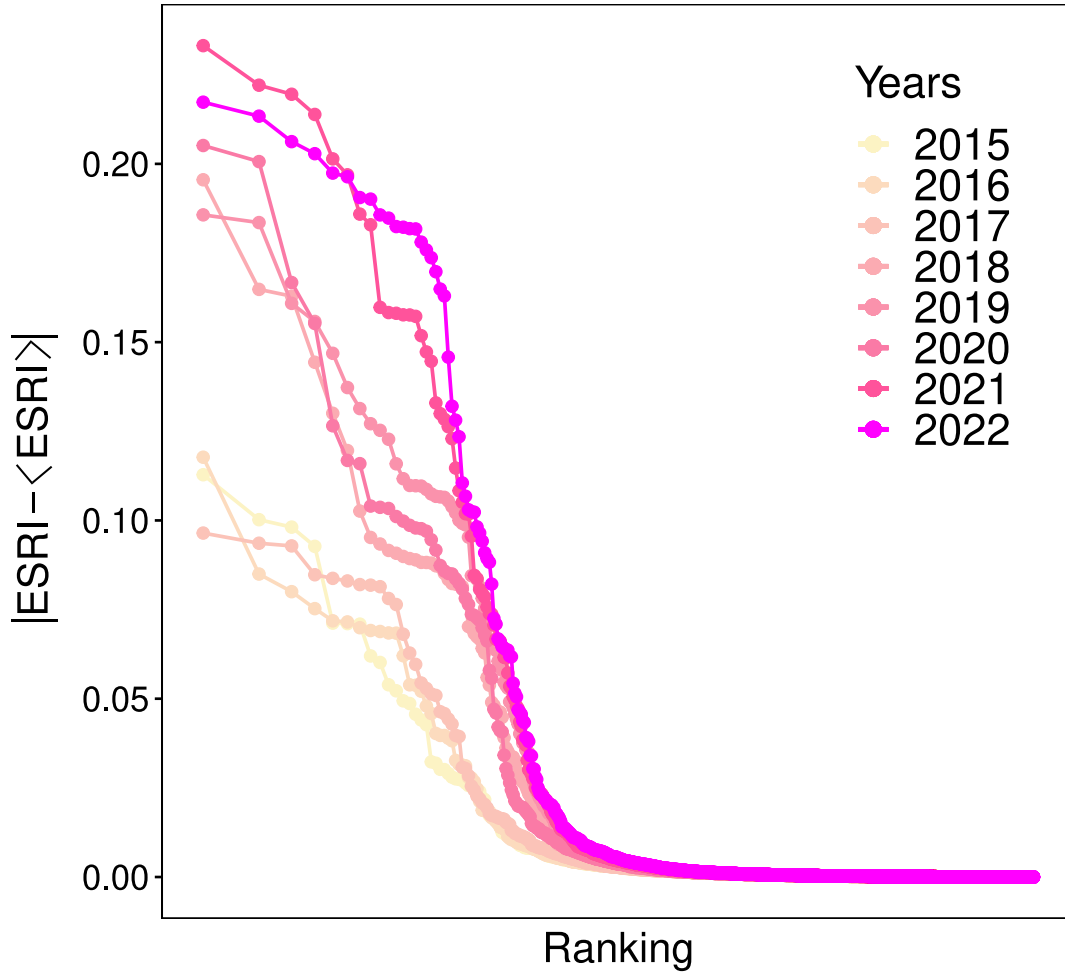


Figure S10. Absolute value of the difference between real and null model ESRI values for all firms, ranked in decreasing order for each year.

S11 Distributions of ESRI values

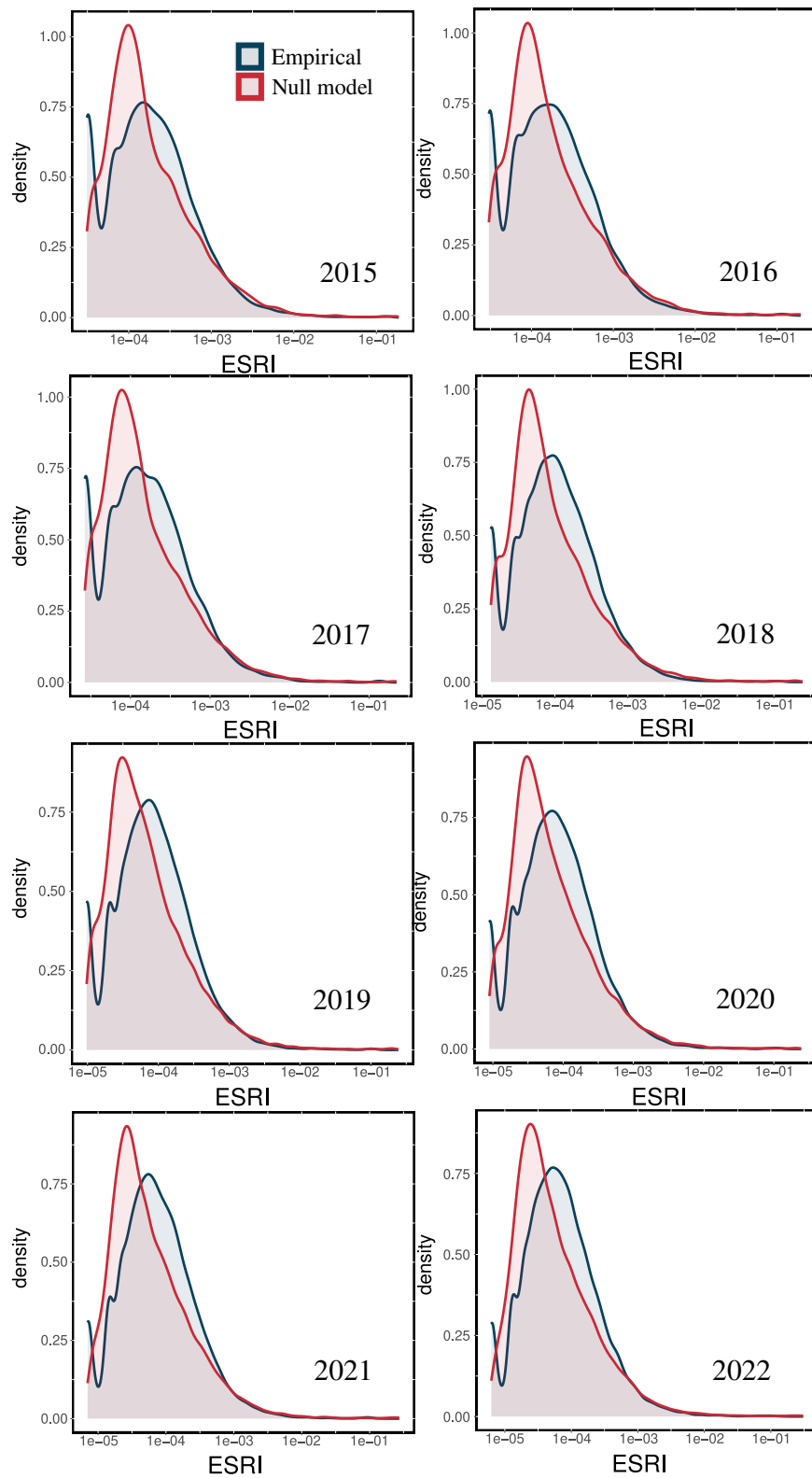


Figure S11. Distributions of ESRI values for all years, for empirical networks (blue) and null models (red).

S12 Sectors of plateaux firms

| NACE4 code | Description |
|------------|---|
| 0812 | Gravel, sand and clay mining |
| 2444 | Manufacture of copper |
| 2572 | Manufacture of locks and hinges |
| 2591 | Manufacture of steel drums and similar containers |
| 2593 | Manufacture of wire products |
| 2612 | Manufacture of loaded electronic boards |
| 2711 | Manufacture of electric motors, generators and transformers |
| 2712 | Manufacture of electricity distribution and control apparatus |
| 2732 | Manufacture of other electronic and electric wires and cables |
| 2733 | Manufacture of assemblies |
| 2740 | Manufacture of electric lighting equipment |
| 2751 | Manufacture of electric domestic appliances |
| 2790 | Manufacture of other electrical equipment |
| 2811 | Manufacture of engines and turbines (except aircraft and cycle engines) |
| 2812 | Manufacture of hydraulic and pneumatic equipment |
| 2815 | Manufacture of bearings, gears, gearing and driving elements |
| 2830 | Manufacture of agricultural and forestry machinery |
| 2849 | Manufacture of other machine tools |
| 2891 | Manufacture of machinery for metallurgy |
| 2895 | Manufacture of machinery for paper and paperboard production |
| 3317 | Repair and maintenance of other transport equipment |
| 3511 | Electricity generation |
| 3512 | Electricity transmission |
| 3513 | Electricity distribution |
| 3514 | Electricity generation from solar energy |
| 3522 | Gas distribution |
| 3523 | Gas trading |
| 3530 | Steam supply, air conditioning |
| 4644 | Wholesale of china and glassware and cleaning materials |
| 4671 | Wholesale of solid, liquid, and gaseous fuels and related products |
| 4672 | Wholesale of metals and metal ores |
| 4931 | Urban and suburban passenger land transport |
| 4910 | Passenger rail transport, interurban |
| 5310 | Postal activity |

Table S12. The 33 NACE4 sectors (codes and descriptions) found in the plateaux of ESRI ranking throughout the years.

S13 Evolution of ESRI plateaux

Figure S13 A displays the ESRI evolution of the top 0.1% of most risky firms that appear in the plateaux of empirical and null model networks more than two years, averaged by NACE2 sectors. The color of each line represents the sector, and the corresponding description can be found in Figure S13 B. Figure S13 C displays the difference of ESRI when a firm last appeared in the plateau compared to when it first appeared. The consistently negative values for the empirical networks imply a decreasing trend, except for the the postal sector, and, to a lesser extent, the manufacture of computers and electronics. These two sectors in fact experienced a growth of their ESRI values during the years, underlining the relevance they gained over time and during the period of crisis and lockdown measures. We can hypothesize that an increasing number of firms (or individuals) bought computers needed for remote work, and incremented the use of courier services to ship and receive items. Instead, all null model sectors, except the manufacture of computers and electronics, show positive variations, implying an increasing trend over time.

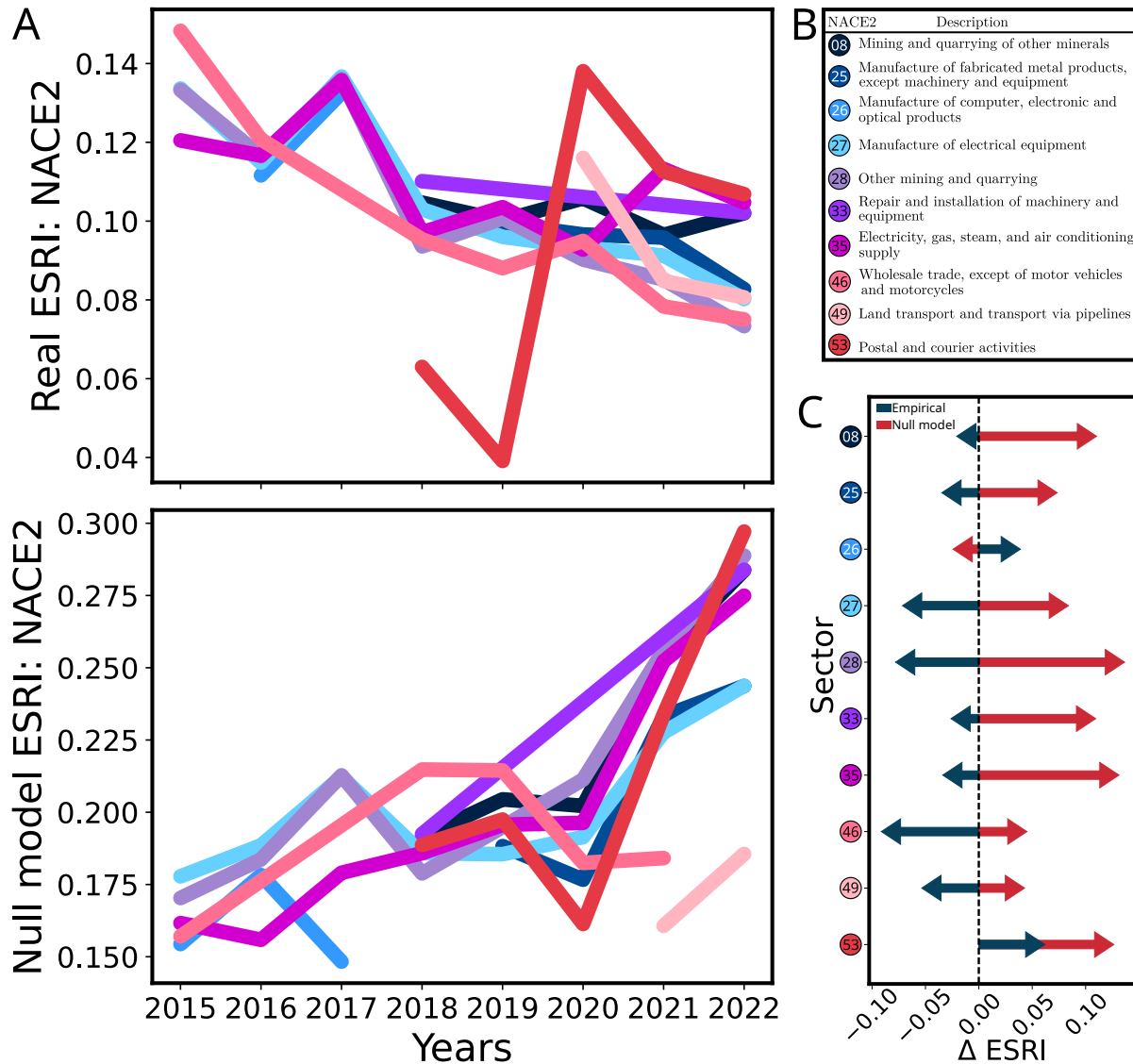


Figure S13. A) Yearly evolution of most risky firms belonging to the plateau for more than two years, present both in empirical and and null model networks, colored by their NACE2 code. Top panel represents empirical values, while bottom panel displays null model values. B) Color legend of NACE2 codes with description. C) Difference between ESRI values of a firm when it last appeared in the plateau and when it first appeared, blue arrows for empirical values and red arrows for null model.

S14 Correlation of firm features

Table S13 summarizes the firm features employed in the regression analysis and what each feature represents. Figure S14 shows the Pearson correlation coefficient between each pair of features, for all years. During COVID years, import and export appear to be less correlated with all of the other variables, as can be expected given the import and export bans introduced to contain the pandemic.

| Feature | Description |
|----------------|--|
| k_{in} | in-degree (number of suppliers) of the firm |
| k_{out} | out-degree (number of customers) of the firm |
| s_{in} | in-strength (total value of purchases) of the firm |
| s_{out} | out-strength (total value of sales) of the firm |
| emp | number of employees of the firm |
| ess | essentiality score of the firm |
| $ESRI$ | empirical ESRI of the firm |
| $ESRI_{model}$ | null model ESRI of the firm |
| $import$ | value of the yearly import of the firm |
| $export$ | value of the yearly export of the firm |

Table S13. Description of the 10 features employed in the regression analysis.

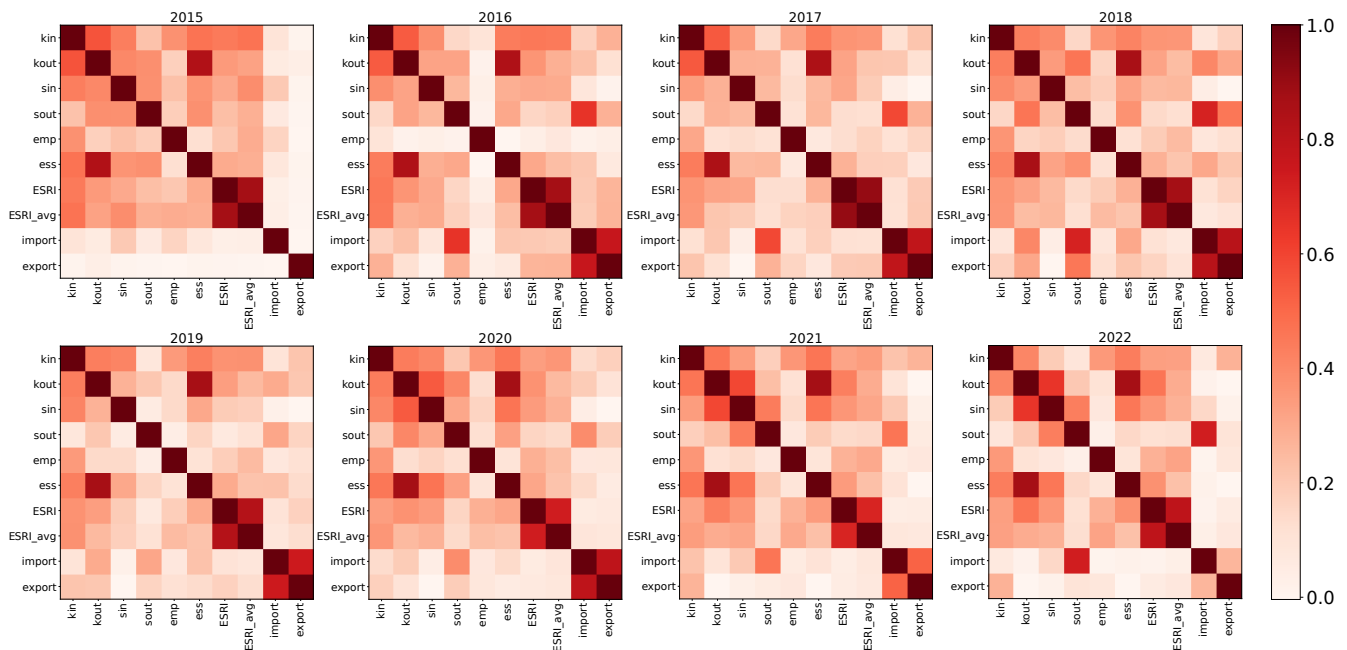


Figure S14. Person correlation coefficients between all pairs of firm variables, throughout the entire time span of data.

S15 Essentiality score vs ESRI

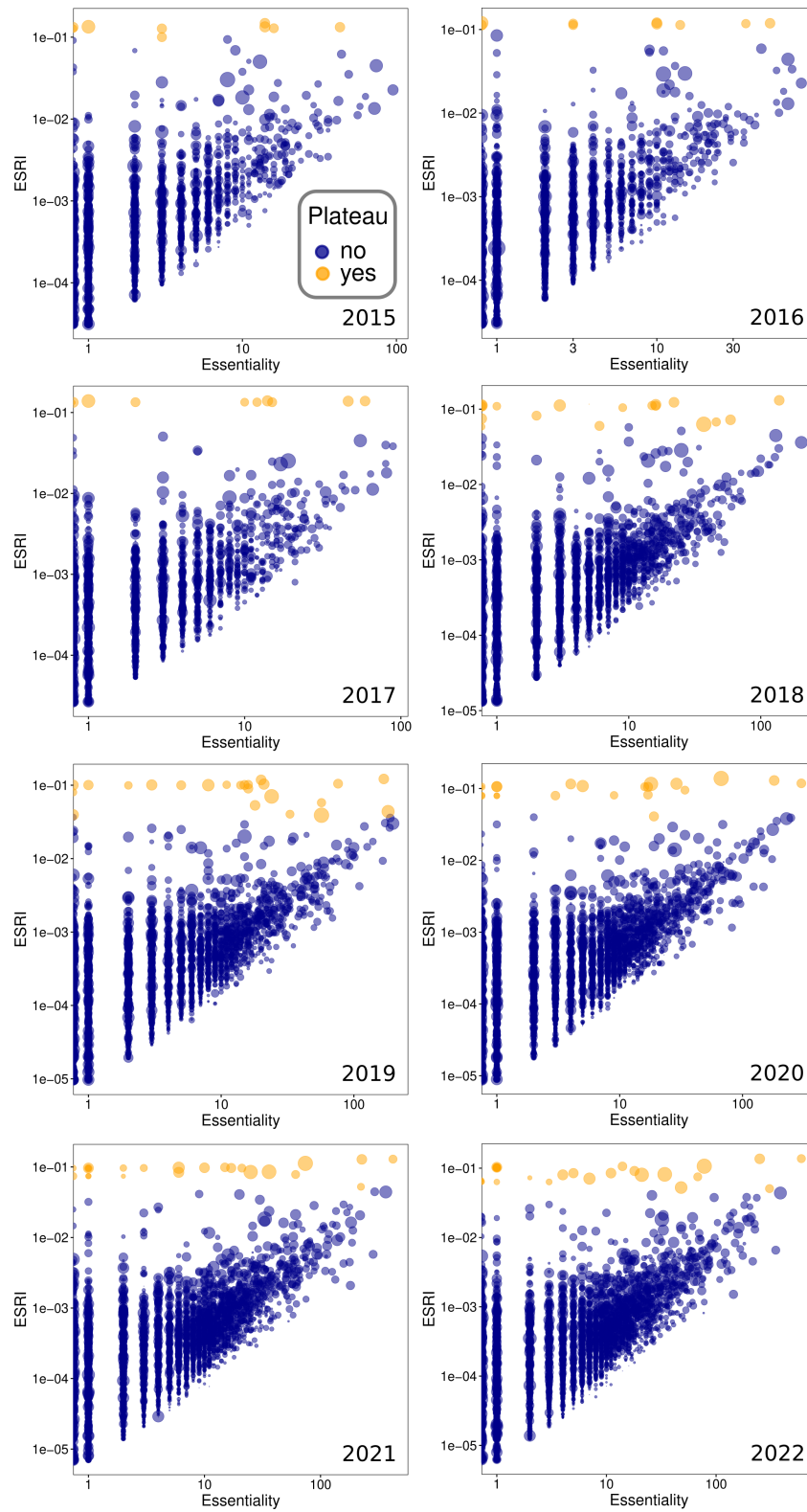


Figure S15. Scatter plot of essentiality score vs ESRI. Dot size is proportional to the firm's out-strength. Orange points are firms that belong to the ESRI plateau of that given year.

S16 Pooled OLS regressions with year fixed effects

| | ESRI | | | | |
|--------------------------------|------------------------------------|-----------------------------------|----------------------------------|----------------------------------|----------------------------------|
| | (1) | (2) | (3) | (4) | (5) |
| <i>ESRI_{model}</i> | 0.733*** (0.002) | 0.724*** (0.002) | 0.704*** (0.002) | 0.696*** (0.002) | 0.684*** (0.002) |
| <i>import</i> | | | | | 0.011*** (0.000) |
| <i>export</i> | | | | | 0.004*** (0.001) |
| <i>emp</i> | | | | 0.027*** (0.002) | 0.009*** (0.002) |
| <i>year = 2016</i> | | 0.000 (0.005) | -0.001 (0.005) | -0.001 (0.005) | -0.010** (0.005) |
| <i>year = 2017</i> | | -0.002 (0.005) | -0.004 (0.005) | -0.004 (0.005) | -0.014*** (0.005) |
| <i>year = 2018</i> | | -0.027*** (0.004) | -0.025*** (0.004) | -0.025*** (0.004) | -0.034*** (0.004) |
| <i>year = 2019</i> | | -0.041*** (0.004) | -0.040*** (0.004) | -0.038*** (0.004) | -0.050*** (0.004) |
| <i>year = 2020</i> | | -0.043*** (0.004) | -0.043*** (0.004) | -0.041*** (0.004) | -0.054*** (0.004) |
| <i>year = 2021</i> | | -0.047*** (0.004) | -0.045*** (0.004) | -0.043*** (0.004) | -0.057*** (0.004) |
| <i>year = 2022</i> | | -0.053*** (0.004) | -0.050*** (0.004) | -0.047*** (0.004) | -0.063*** (0.004) |
| Constant | -1.018*** (0.006) | -1.023*** (0.007) | -1.276*** (0.043) | -1.338*** (0.043) | -1.364*** (0.043) |
| Observations | 160,895 | 160,895 | 160,895 | 157,612 | 157,612 |
| <i>R</i> ² | 0.587 | 0.588 | 0.614 | 0.618 | 0.621 |
| Adjusted <i>R</i> ² | 0.587 | 0.588 | 0.613 | 0.617 | 0.620 |
| Residual Std. Error | 0.364 (df = 160893) | 0.363 (df = 160886) | 0.352 (df = 160325) | 0.351 (df = 157041) | 0.350 (df = 157039) |
| F Statistic | 228,593.900*** (df = 1; 160893) | 28,694.400*** (df = 8; 160886) | 448.369*** (df = 569; 160325) | 446.290*** (df = 570; 157041) | 450.000*** (df = 572; 157039) |

Table S16. Pooled OLS regressions with year fixed effects. *** Significant at the 1% level. ** Significant at the 5% level. * Significant at the 10% level.

S17 Cross-sectional regressions for import

| | ESRI | | | | | | | |
|--------------------------------|-------------------------------|-------------------------------|-------------------------------|--------------------------------|--------------------------------|--------------------------------|--------------------------------|--------------------------------|
| | (1) | (2) | (3) | (4) | (5) | (6) | (7) | (8) |
| <i>ESRI_{model}</i> | 0.425*** (0.016) | 0.399*** (0.016) | 0.371*** (0.015) | 0.379*** (0.011) | 0.373*** (0.011) | 0.389*** (0.011) | 0.372*** (0.010) | 0.350*** (0.010) |
| <i>import</i> | -0.003 (0.009) | 0.010 (0.007) | 0.010 (0.007) | 0.021*** (0.006) | 0.027*** (0.006) | 0.034*** (0.006) | 0.034*** (0.005) | 0.020*** (0.005) |
| <i>sout</i> | -0.017 (0.011) | -0.001 (0.011) | 0.022** (0.010) | 0.033*** (0.008) | 0.048*** (0.008) | 0.043*** (0.008) | 0.052*** (0.008) | 0.054*** (0.008) |
| <i>sin</i> | 0.049*** (0.002) | 0.045*** (0.002) | 0.045*** (0.002) | 0.038*** (0.001) | 0.038*** (0.001) | 0.040*** (0.001) | 0.039*** (0.001) | 0.045*** (0.001) |
| <i>ess</i> | 0.529*** (0.017) | 0.522*** (0.019) | 0.513*** (0.017) | 0.488*** (0.012) | 0.475*** (0.011) | 0.472*** (0.011) | 0.473*** (0.010) | 0.479*** (0.010) |
| <i>emp</i> | -0.006 (0.007) | -0.022*** (0.007) | -0.017*** (0.006) | -0.007 (0.005) | 0.012** (0.005) | 0.003 (0.005) | 0.005 (0.005) | 0.015*** (0.005) |
| <i>plateau</i> | 1.200*** (0.135) | 1.183*** (0.131) | 1.082*** (0.138) | 1.083*** (0.090) | 0.897*** (0.080) | 1.143*** (0.089) | 1.160*** (0.092) | 1.191*** (0.089) |
| <i>import : sout</i> | 0.000 (0.002) | -0.000 (0.002) | -0.001 (0.002) | -0.006*** (0.001) | -0.006*** (0.001) | -0.008*** (0.001) | -0.009*** (0.001) | -0.007*** (0.001) |
| <i>import : sin</i> | 0.001 (0.001) | 0.001* (0.000) | 0.002*** (0.000) | 0.003*** (0.000) | 0.002*** (0.000) | 0.002*** (0.000) | 0.004*** (0.000) | 0.004*** (0.000) |
| <i>import : ess</i> | 0.006 (0.004) | -0.002 (0.004) | -0.004 (0.004) | 0.002 (0.003) | 0.002 (0.002) | 0.006*** (0.002) | 0.004** (0.002) | 0.003 (0.002) |
| <i>Constant</i> | -2.714*** (0.176) | -2.655*** (0.252) | -2.785*** (0.210) | -2.858*** (0.180) | -3.218*** (0.132) | -2.976*** (0.129) | -3.208*** (0.134) | -3.259*** (0.125) |
| Observations | 9,000 | 9,253 | 10,308 | 16,474 | 20,604 | 21,579 | 24,909 | 25,829 |
| <i>R</i> ² | 0.630 | 0.613 | 0.623 | 0.622 | 0.631 | 0.630 | 0.630 | 0.642 |
| Adjusted <i>R</i> ² | 0.609 | 0.592 | 0.605 | 0.610 | 0.621 | 0.621 | 0.622 | 0.634 |
| Residual Std. Error | 0.318 (df = 8522) | 0.322 (df = 8783) | 0.318 (df = 9835) | 0.320 (df = 15963) | 0.317 (df = 20087) | 0.321 (df = 21060) | 0.328 (df = 24378) | 0.329 (df = 25299) |
| F Statistic | 30.375*** (df = 477; 8522) | 29.662*** (df = 469; 8783) | 34.504*** (df = 472; 9835) | 51.526*** (df = 510; 15963) | 66.464*** (df = 516; 20087) | 69.282*** (df = 518; 21060) | 78.276*** (df = 530; 24378) | 85.638*** (df = 529; 25299) |

Table S17. Cross sectional regressions for import. *** Significant at the 1% level. ** Significant at the 5% level. * Significant at the 10% level.

S18 Cross-sectional regressions for export

| | ESRI | | | | | | | |
|---------------------------------|-------------------------------|-------------------------------|-------------------------------|--------------------------------|--------------------------------|--------------------------------|--------------------------------|--------------------------------|
| | (1) | (2) | (3) | (4) | (5) | (6) | (7) | (8) |
| <i>ESRI_{model}</i> | 0.427*** (0.016) | 0.395*** (0.016) | 0.369*** (0.015) | 0.380*** (0.011) | 0.371*** (0.011) | 0.387*** (0.011) | 0.371*** (0.010) | 0.354*** (0.010) |
| <i>export</i> | -0.031 (0.021) | -0.016* (0.009) | -0.008 (0.009) | 0.003 (0.008) | 0.007 (0.008) | 0.012*** (0.008) | 0.015** (0.008) | 0.000 (0.007) |
| <i>s_{out}</i> | -0.018* (0.010) | 0.000 (0.011) | 0.023** (0.010) | 0.027*** (0.008) | 0.045*** (0.008) | 0.038*** (0.008) | 0.046*** (0.008) | 0.046*** (0.008) |
| <i>s_{in}</i> | 0.050*** (0.002) | 0.045*** (0.002) | 0.046*** (0.002) | 0.040*** (0.001) | 0.039*** (0.001) | 0.041*** (0.001) | 0.041*** (0.001) | 0.047*** (0.001) |
| <i>ess</i> | 0.541*** (0.016) | 0.534*** (0.017) | 0.522*** (0.016) | 0.498*** (0.012) | 0.478*** (0.010) | 0.481*** (0.010) | 0.479*** (0.009) | 0.483*** (0.009) |
| <i>emp</i> | -0.004 (0.007) | -0.011* (0.007) | -0.008 (0.006) | -0.003 (0.005) | 0.017*** (0.005) | 0.007 (0.005) | 0.011** (0.005) | 0.021*** (0.005) |
| <i>plateau</i> | 1.176*** (0.135) | 1.138*** (0.132) | 1.078*** (0.138) | 1.063*** (0.090) | 0.853*** (0.081) | 1.140*** (0.089) | 1.153*** (0.092) | 1.179*** (0.089) |
| <i>export : s_{out}</i> | 0.006 (0.005) | 0.003 (0.002) | 0.002 (0.002) | -0.002 (0.002) | -0.004** (0.002) | -0.005*** (0.002) | -0.006*** (0.002) | -0.004*** (0.002) |
| <i>export : s_{in}</i> | 0.001 (0.002) | 0.003*** (0.001) | 0.003*** (0.001) | 0.004*** (0.001) | 0.005*** (0.001) | 0.004*** (0.001) | 0.005*** (0.001) | 0.005*** (0.001) |
| <i>export : ess</i> | -0.006 (0.013) | -0.009* (0.005) | -0.011** (0.004) | -0.005 (0.004) | -0.000 (0.003) | 0.003 (0.003) | 0.002 (0.003) | 0.003 (0.003) |
| <i>Constant</i> | -2.707*** (0.176) | -2.695*** (0.253) | -2.811*** (0.210) | -2.838*** (0.180) | -3.223*** (0.132) | -2.962*** (0.129) | -3.199*** (0.134) | -3.217*** (0.126) |
| Observations | 9,000 | 9,253 | 10,308 | 16,474 | 20,604 | 21,579 | 24,909 | 25,829 |
| <i>R</i> ² | 0.629 | 0.611 | 0.622 | 0.621 | 0.630 | 0.629 | 0.629 | 0.640 |
| Adjusted <i>R</i> ² | 0.609 | 0.591 | 0.604 | 0.609 | 0.621 | 0.620 | 0.621 | 0.633 |
| Residual Std. Error | 0.318 (df = 8522) | 0.323 (df = 8783) | 0.318 (df = 9835) | 0.321 (df = 15963) | 0.318 (df = 20087) | 0.322 (df = 21060) | 0.328 (df = 24378) | 0.330 (df = 25299) |
| F Statistic | 30.325*** (df = 477; 8522) | 29.449*** (df = 469; 8783) | 34.290*** (df = 472; 9835) | 51.360*** (df = 510; 15963) | 66.329*** (df = 516; 20087) | 69.002*** (df = 518; 21060) | 77.851*** (df = 530; 24378) | 85.192*** (df = 529; 25299) |

Table S18. Cross sectional regressions for export. *** Significant at the 1% level. ** Significant at the 5% level. * Significant at the 10% level.